# Geometry and mechanics of uniform $n$-plies: from engineering ropes to biological filaments

S. Neukirch

Bernoulli Institute

Swiss Federal Institute of Technology

Lausanne, CH-1015, Switzerland

sebastien.neukirch@epfl.ch

G.H.M. van der Heijden

Centre for Nonlinear Dynamics

University College London

London WC1E 6BT, UK

g.heijden@ucl.ac.uk

## Abstract

We study the mechanics of uniform $n$-plies, correcting and extending previous work in the literature. An $n$-ply is the structure formed when $n$ pretwisted strands coil around one another in helical fashion. Such structures are encountered widely in engineering (mooring ropes, power lines) and biology (DNA, proteins). We first show that the well-known lock-up phenomenon for $n = 2$, described by a pitchfork bifurcation, gets unfolded for higher $n$. Geometrically, $n$-plies with $n > 2$ are all found to behave qualitatively the same. Next, using elastic rod theory, we consider the mechanics of $n$-plies, allowing for axial end forces and end moments while ignoring friction. An exact expression for the interstrand pressure force is derived, which is used to investigate the onset of strand separation in plied structures. After defining suitable displacements we also give an alternative variational formulation and derive (nonlinear) constitutive relationships for torsion and extension (including their coupling) of the overall ply. For a realistic loading problem in which the ends are not free to rotate one needs to consider the topological conservation law, and we show how the concepts of link and writhe can be extended to $n$-plies.

**Keywords**: multi-strand plies, rod mechanics, end loads, constitutive relations, twist-stretch coupling, strand separation, birdcaging, helix, link, writhe, wire rope, DNA, proteins

# 1 Introduction

Plies consisting of two strands of elastic tube (rod) winding around each other while contacting along a straight line have recently been studied using rod theory, especially in the context of DNA supercoiling. Both the uniform [39] and the variable-angle ply [7] have been treated. In [40] the loaded ply was considered and some simple constitutive relations for the ply were derived. It was also observed that under increasing pretwist in its individual strands, the helical angle of the

1

(infinitely long and uniform) ply tends to a limiting value of $\pi/4$. This is exactly the lock-up angle for a double helix with straight-line contact: a larger angle would lead to self-penetration of the rod [30, 36].

In [45] numerical computations on a clamped finite-length variable ply showed that the variation of the ply angle in an end-loaded ply is small, but also that due to bending boundary layers at the clamped ends, lock-up occurs at the clamps long before the $\pi/4$ angle is reached. In fact, there are two possible effects of the thickness of the rod. One local: the centreline cannot be bent too sharply (the local radius of curvature cannot be smaller than the radius of the rod). One global: any two points far apart along the rod cannot come too close to each other in space (not closer than twice the radius of the rod). If either of these is violated the tube suffers self-penetration. The two conditions are neatly combined into a single one by introducing the concept of the global radius of curvature as defined by Gonzalez & Maddocks [17]. Many of the issues relevant for plies also arise in tightly wound single helices (1-plies) as studied in, e.g., [31].

In this paper we study a wider class of plies in order to understand this lock-up phenomenon better. In particular we shall drop the requirement that the strands in the ply touch along a straight line. This leads us naturally to consider plies made up of an arbitrary number of strands. It then turns out that the limiting angle at large twist has really nothing to do with the lock-up angle. They just happen to be the same. For $n > 2$ the limiting angle still occurs, while the lock-up angle gets unfolded and disappears.

A common way to form a ply is to take a few strands of elastic material, hold them under tension while putting a number of turns into each of them individually, and then to reduce the tension thereby letting the strands writhe around themselves. By adopting a writhed configuration the strands release torsional energy (by reducing their twist) at the expense of bending energy (by increasing their curvature). However, if the ends are prevented from rotation, then there is a topological conserved quantity analogous to the constant linking number of a closed rod undergoing arbitrary deformations. Indeed, we show how this linking number, which is numerically equal to the sum of the 'twist' and the 'writhe', can be adapted for $n$-plies.

Plied structures, consisting of multiple fibres or wires winding around one another are found in a wide class of engineering components, and also occur widely in molecular biology. Although the length scales in these two application areas are vastly different, the main function of plied structures in many cases is the same, namely, to support large axial loads with comparatively small bending and torsional stiffness. One area where ply formation has traditionally been important is textile engineering, and there is a relatively old literature, including experimental studies, on twisted yarn [41, 19, 12, 13]. In offshore engineering wire rope (mostly consisting of 6 wires wound around a core) is used in mooring lines [6]. In biology, the fibrous protein collagen, the most abundant protein in the animal kingdom, occurs in the form of 3-plies. This form makes it suitable for its primary purpose, which is to help tissues withstand stretching [28]. Artificial DNA in the form of 3-plies, and even 4-plies, is also used in genetic engineering [16, 46, 22]. Plies with six strands, wound around a seventh one, occur in keratin, another class of mechanical support proteins. Proteins lining ion channels in cell membranes are also arranged in hexagonal form; see [48] and references therein. In this case the structure is supported by electrostatic forces and

2

there is no central core. In some models the diameter of the channel is controlled by twisting the molecules, i.e., changing the angle of the ply they form [42].

Since the mechanics of plies is one of large deformation geometric rod models have been used widely. In almost all cases helical shapes for the individual strands are assumed. For an overview of work in this direction we refer to the book by Costello [8] and the recent survey article by Cardou & Jolicœur [5]. However, in all studies we are aware of the contact problem is studied in a plane normal to the ply axis. This is too simplistic an approach and cannot ensure that the structure does not suffer self-penetration further down the ply (cf. the lock-up angle mentioned above). Here we correct and extend this work on $n$-ply geometry by showing that the helical strands generally interact in an intrinsically three-dimensional way: contacting sections of neighbouring strands are generally not in the same normal cross-section of the overall ply. While still assuming helical shapes for the strands, we take proper account of the ply geometry in order to avoid self-penetration. This leads to a different relationship between ply diameter and ply angle.

Next we use elastic rod theory to study the mechanics of the problem. We model a strand as a perfect, isotropic rod, i.e., an intrinsically straight rod with equal bending stiffnesses about its principal axes. A semi-inverse approach is taken in which we *assume* helical shapes for the centrelines of the strands and then use the static equilibrium equations to obtain new expressions for the forces and moments in the ply, including the pressure force acting between the strands (which in general is not normal to the ply axis). By allowing for end forces and end twisting moments we are then in a position to examine the onset of strand separation, defined as the point where the interstrand pressure vanishes. This could be relevant for the study of 'birdcaging', the phenomenon in which, under compression or counterrotation, the individual strands buckle locally and separate, thereby opening up the ply. Birdcaging may lead to a dramatic reduction in strength and is an important failure mode in engineering ropes [6]. An analogous phenomenon in molecular biology is the (local) unzipping (denaturation or 'melting') of the DNA double helix, either thermally [29] or force-induced [10, 3, 32]. DNA is also known to undergo structural transitions under applied stresses [1, 33] or in complexes with proteins and other ligands.

Finally, we give a self-contained variational formulation of $n$-ply mechanics and derive (nonlinear) constitutive relationships between the applied loads and the extension and rotation of the overall ply. In particular we compute the effective torsional and axial stiffnesses, as well as the twist-stretch coupling stiffnesses. Costello's book [8] gives a simplified treatment of bending constitutive behaviour of plies. An exact analysis using rod theory is more complicated and left for future work. The effective stiffnesses could be used as building blocks for more complicated plied structures.

There have been different approaches to studying plied structures. In [27] a (dynamical) composite rod theory is developed that can describe 2-plies whose strands may have arbitrary configurations. This is used to derive nonlinear as well as linear constitutive relations. In [30] the geometry of $n$-plies is considered numerically using a kind of simulated annealing. Similar techniques have led to the related study of so-called ideal shapes of knotted curves [23, 35, 17]. In [20] plies with more complicated cross-sections made up of layers of helical components are

3

considered, using rod theory for each of these components. Multi-layered plies have also been investigated using finite-element computations [21].

# 2   The geometry of $n$-plies

Consider a ply made up of $n$ strands of radius $r$ winding as helices on a cylinder of radius $R$. The strands are modelled as impenetrable elastic tubes of uniform circular cross-section obeying the special case of the Kirchhoff theory of elastic rods in which a rod is taken to be not only transversely isotropic but also inextensible and unshearable [9]. Thus all material cross-sections form circular discs of radius $r$.

Let $\{e_1, e_2, e_3\}$ be a fixed right-handed orthonormal co-ordinate frame. Relative to this frame the centreline of one of the strands can be written as

$$r_1(s) = \begin{pmatrix} +\epsilon R \, \sin \psi(s) \\ -\epsilon R \, \cos \psi(s) \\ s \, \cos \theta \end{pmatrix}, \qquad \psi'(s) = \frac{\epsilon \sin \theta}{R}, \qquad \psi(0) = 0, \tag{1}$$

where $s$ denotes arclength along the centreline and $' = d/ds$. The angle $\theta$ is the helical angle, the complement of what is usually called the pitch angle. We use $\epsilon$ to designate the handedness of the helix: $\epsilon = 1$ for a right-handed helix, $\epsilon = -1$ for a left-handed helix. We shall therefore assume $\theta$ to lie in the range $[0, \pi/2]$. The centrelines of all the other strands in the ply are given by

$$r_{i+1} = \mathcal{R}_n^i \, r_1 \qquad (i = 1, ..., n-1), \tag{2}$$

where $\mathcal{R}_n$ is the matrix

$$\mathcal{R}_n = \begin{pmatrix} \cos \frac{2\pi}{n} & -\sin \frac{2\pi}{n} & 0 \\ \sin \frac{2\pi}{n} & \cos \frac{2\pi}{n} & 0 \\ 0 & 0 & 1 \end{pmatrix}, \tag{3}$$

describing a rotation through $2\pi/n$ about $e_3$.

Contact between two strands, $r_1$ and $r_2$ say, is governed by two geometrical conditions. If strand 1, at arclength $s_1$, touches strand 2, at arclength $s_2$, then we must have:

C1. $|r_1(s_1) - r_2(s_2)| = 2r$ (the interstrand distance must be equal to the diameter of the rod).

C2. $r_1'(s_1) \cdot (r_1(s_1) - r_2(s_2)) = r_2'(s_2) \cdot (r_1(s_1) - r_2(s_2)) = 0$ (the tangent to either strand must be orthogonal to the line connecting the two centreline points at contact).

These conditions give the following two equations:

$$\Delta(\theta, x) := 2 + x^2 \cos^2 \theta - 2 \cos \left( x \sin \theta - \frac{2\pi}{n} \right) = \frac{4}{\rho^2}, \tag{4}$$

$$x \cos^2 \theta + \sin \theta \, \sin \left( x \sin \theta - \frac{2\pi}{n} \right) = 0, \tag{5}$$

4

where

$$x = \frac{\epsilon(s_1 - s_2)}{R}, \qquad \rho = \frac{R}{r}. \tag{6}$$

Note the translation invariance: both conditions depend on $s_1$ and $s_2$ only through $x$ (indeed, the two tangency conditions C2 yield identical equations). With the factor $\epsilon$ as included in the definition of $x$, given a right-handed solution, a left-handed one is obtained simply by reversing the roles of $s_1$ and $s_2$. For $n = 2$ the equations are additionally invariant under a sole sign change of $x$. Also note that (5) is just the statement $\partial\Delta(\theta, x)/\partial x = 0$, reflecting the fact that we are minimising the interstrand distance (at fixed $\theta$).

The reason for using the (initially unknown) ply radius $R$ in the definition of $x$ in (6) is that the equations (4) and (5) have a simple form, with $\rho$ appearing only in the first. The natural interpretation of the problem is that $n$, $r$ and $\theta$ are given, that $x$ then follows from (5), and then $R$ from (4) and (6).

When the strands are straight, $\theta = 0$, (5) yields $x = 0$, whereupon (4) gives

$$\rho = 1/\sin\frac{\pi}{n}, \tag{7}$$

which is the result one gets when studying tangency of $n$ circles whose centres lie on a circle. In the other limit, $\theta \to \pi/2$, where the strands become rings, (5) gives $x = 2\pi/n$ and (4) shows that $\rho \to \infty$.

Before we turn to the analysis of the equations (4) and (5) for real plies, note that the case $n = 1$ is of interest as well. For instance, the local curvature of the helical strand is given by $\sin^2\theta/R$ and this cannot exceed $1/r$. If we use $\rho = \sin^2\theta$ in (4) we find the solution

$$\theta = 1.190458 \ \ (68.2082°), \qquad x = 5.685134, \qquad \rho = 0.862185, \tag{8}$$

which is the densest packing solution of a single helical tube [26, 31]. This solution simultaneously satisfies both the local and the global thickness constraint mentioned in the Introduction.

## 2.1   The case $n = 2$

Fig. 1 gives a graphical representation of (5) for $n = 2$. There is a trivial solution $x = 0$ for all values of $\theta$: contact occurs at the same arclength along both strands. This solution has $\rho = 1$ and is the one studied in previous work [12, 7, 40, 45]. As can easily be established from (5), at $\theta = \frac{\pi}{4}$ a non-trivial path ($x \neq 0$) bifurcates from the trivial one [36]. The corresponding solutions have $\rho > 1$, implying that they have a central hole of radius $R - r$ (see Fig. 2).

The trivial solution corresponds to the global minimum of the interstrand distance function $\Delta$ only for $\theta < \pi/4$. For larger angles the bifurcating solution takes over that role, and the $x = 0$ solution has self-penetrations. The non-bifurcating 'satellite' solutions further out in Fig. 1 never correspond to global minima and therefore always have self-penetrations (partly they also violate the local curvature condition $\sin^2\theta \leq \rho$).

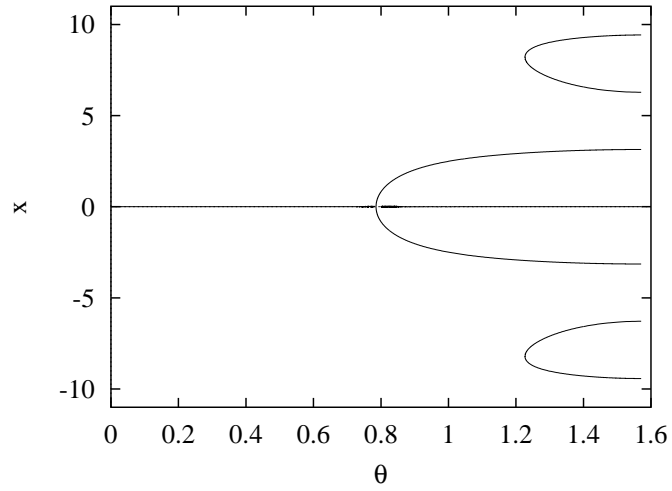Related but different aspects of 2-ply geometry are described in [18].

Figure 1: Arclength shift $x$ versus helical angle $\theta$ for $n = 2$ as given by (5). The trivial branch $x = 0$ represents plies whose strands are touching on a straight line; the non-trivial branches represent plies whose strands are touching on a helix.
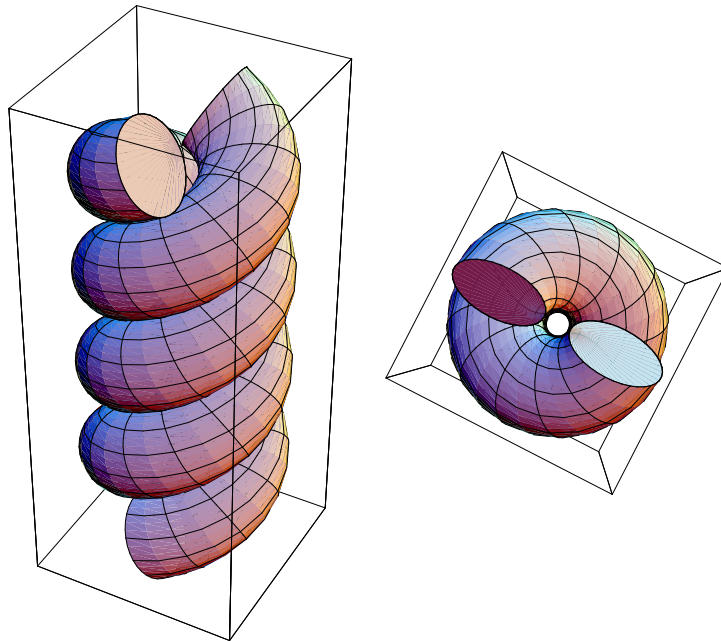


Figure 2: Two views of a 2-ply with $\theta > \pi/4$ along the non-trivial branch in Fig. 1 ($\theta = 60°$).
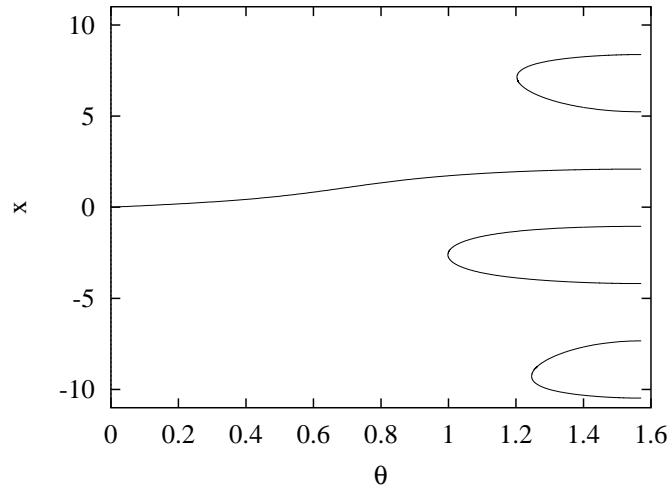
6

Figure 3: Arclength shift $x$ versus helical angle $\theta$ for $n = 3$ as given by (5). Only the main branch through the origin contains non-self-penetrating solutions.
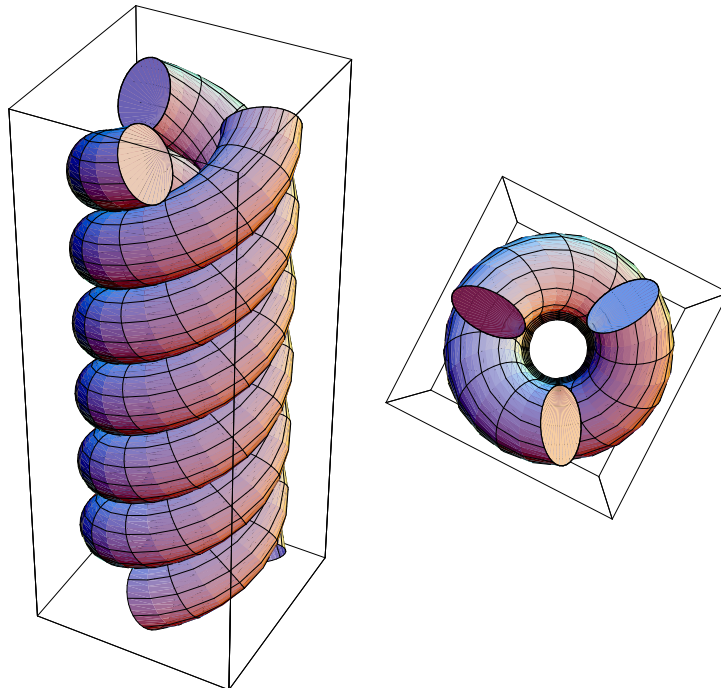


Figure 4: Two views of a 3-ply along the main branch in Fig. 3 ($\theta = 60°$).

## 2.2 The case $n = 3$ and higher

For $n = 3$ the solution $x = 0$ no longer exists for non-zero $\theta$ and there is no bifurcation (see Fig. 3). In fact, the $\theta$-$x$ diagram can be interpreted as an unfolding of the pitchfork bifurcation in Fig. 1 with $\lambda := 2\pi/n$ as imperfection parameter (imagined continuous). All 3-plies have central holes (see Fig. 4). The main branch contains the global minima of $\Delta$ and for these solutions the local curvature does not exceed $1/r$.

For $n > 3$ the results remain qualitatively the same as for $n = 3$.

The fact that $n$-plies for $n > 2$ have solutions with $x \neq 0$, i.e., with an arclength shift between touching sections, implies that the simple analyses in [13, 8], where single cross-sections of the ply are considered, are only valid for small $\theta$. In [8] strand cuts normal to the ply axis are taken to be elliptical, while in [13] the varying orientation of the cross-sections as a result of the curvature is not even considered, so that (7) is simply obtained, a result which is only true for straight strands! In [24] it is pointed out that for tightly layed ropes the normal strand cut can deviate significantly from being elliptical, but the authors continue to make the same mistake by focussing on a single ply cross-section rather than considering the helical structure as a whole. Consequently, all these analyses yield solutions that in reality would have self-penetrations.

In fact, it is instructive to see what a ply cut does look like. A parametrisation of the perimeter of a single strand can be obtained as follows. For the position vector $\boldsymbol{r}_s$ of a point on the surface of the rod we can write the parametrisation

$$\boldsymbol{r}_s(s, \alpha) = \boldsymbol{r}_1(s) + r \sin \alpha \, \boldsymbol{n} + r \cos \alpha \, \boldsymbol{b}, \tag{9}$$

where $\alpha \in [0, 2\pi]$ is the angle along the circumference of the material cross-section at arclength $s$, and $\boldsymbol{n} = \boldsymbol{r}_1''/|\boldsymbol{r}_1''|$ and $\boldsymbol{b} = \boldsymbol{r}_1' \times \boldsymbol{n}$ are the normal and binormal of the strand's centreline, respectively. With (1) this becomes

$$\boldsymbol{r}_s(s, \alpha) = \begin{pmatrix} x_s \\ y_s \\ z_s \end{pmatrix} = \epsilon \begin{pmatrix} R \sin \psi - r \sin \alpha \sin \psi - r \cos \alpha \cos \theta \cos \psi \\ -R \cos \psi + r \sin \alpha \cos \psi - r \cos \alpha \cos \theta \sin \psi \\ \epsilon s \cos \theta + r \cos \alpha \sin \theta \end{pmatrix}, \quad \psi = \frac{\epsilon s \sin \theta}{R}. \tag{10}$$

For a cut normal to the ply axis we have $z_s = z_0$, for some constant $z_0$, which can be used to solve for $s$ in (10) to get

$$s = \frac{z_0 - \epsilon r \cos \alpha \sin \theta}{\cos \theta}. \tag{11}$$

Insertion of this back into (10) gives the sought parametrisation $(x_s(\alpha), y_s(\alpha))$. (11) gives the arclength co-ordinate of the material cross-section that the point on the cut at given $\alpha$ belongs to. Fig. 5 shows cuts of 3-plies with different helical angles. For sufficiently large $\theta$ (for $n = 3$, $> 51.2°$) the strand cut becomes non-convex.

## 2.3 The contact curve is a helix

We have seen that for $\theta > \pi/4$ if $n = 2$ and for $\theta > 0$ if $n > 2$ the non-self-penetrating solution has an arclength shift $x$. As a result the contact curve is no longer a straight line and the ply has a hole in the centre. It is straightforward to show that the contact curve is in fact itself a helix.
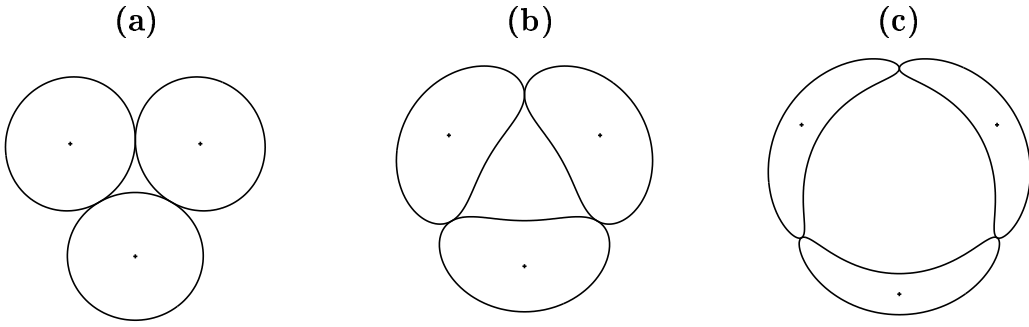
8

Figure 5: Cut at $z_s = 0$ of a 3-ply with (a) $\theta = 20°$, (b) $\theta = 60°$ and (c) $\theta = 80°$.

Fix a point $\boldsymbol{r}_1(s_1)$ on the centreline of strand 1. The cross-section at this point will touch the cross-section at $\boldsymbol{r}_2(s_2)$ of the neighbouring strand 2, where $s_2 = s_1 - \epsilon R x$. The contact point $\boldsymbol{r}_c$ between the strands will be the midpoint of the line segment from $\boldsymbol{r}_1(s_1)$ to $\boldsymbol{r}_2(s_2)$:

$$\boldsymbol{r}_c = \frac{1}{2}\left(\boldsymbol{r}_1(s_1) + \boldsymbol{r}_2(s_1 - \epsilon R x)\right). \tag{12}$$

(Here we imagine an infinitely long ply so that end effects can be ignored.) Note that with the two tangency conditions C2 there is still the freedom for the two contacting cross-sections to rotate relative to each other about the line through both $\boldsymbol{r}_1(s_1)$ and $\boldsymbol{r}_2(s_2)$, so the tangents $\boldsymbol{r}_1'(s_1)$ and $\boldsymbol{r}_2'(s_2)$ need not be aligned.

Using (1) and (2) we obtain

$$\boldsymbol{r}_c = \begin{pmatrix} \epsilon R \cos\left(\frac{1}{2}x\sin\theta - \frac{\pi}{n}\right) \sin\left[\psi(\frac{1}{2}(s_1 + s_2)) + \frac{\pi}{n}\right] \\ -\epsilon R \cos\left(\frac{1}{2}x\sin\theta - \frac{\pi}{n}\right) \cos\left[\psi(\frac{1}{2}(s_1 + s_2)) + \frac{\pi}{n}\right] \\ \frac{1}{2}(s_1 + s_2)\cos\theta \end{pmatrix}. \tag{13}$$

This represents a helix, parametrised by $\frac{1}{2}(s_1 + s_2)$, of radius $R\cos\left(\frac{1}{2}x\sin\theta - \frac{\pi}{n}\right)$ and of the same helical angle as the two strands.

# 3   The mechanics of $n$-plies

In this section we study the mechanics of the ply. For this it will be necessary to consider the amount of twist in the strands. We use the Cosserat director theory of elastic rods [2], which besides the centreline of the rod, $\boldsymbol{r}$, defines a right-handed orthonormal frame $\{\boldsymbol{d}_1, \boldsymbol{d}_2, \boldsymbol{d}_3\}$ (the directors) at each point along the rod. This frame allows one to describe arbitrary orientations of the cross-section of the rod, including twist.

In the following we shall use $\boldsymbol{r}$ for the centreline when no particular strand is meant and refer to the strand as 'the rod'.

For simplicity we shall assume the rod to be inextensible and unshearable (an adequate assumption in most applications) so that we can choose $\boldsymbol{d}_3(s)$ to be the unit tangent to the

9

centreline at $s$, while $\boldsymbol{d}_1(s)$ and $\boldsymbol{d}_2(s)$ span the normal cross-section at $s$:

$$\boldsymbol{r}' = \boldsymbol{d}_3. \tag{14}$$

We can parametrise $\boldsymbol{d}_3$ by two angles as follows:

$$\boldsymbol{d}_3 = \begin{pmatrix} \sin\theta \cos\psi \\ \sin\theta \sin\psi \\ \cos\theta \end{pmatrix}. \tag{15}$$

At this point the angles are arbitrary functions of $s$. The evolution of the director frame along the rod is governed by

$$\boldsymbol{d}_i' = \boldsymbol{u} \times \boldsymbol{d}_i \qquad (i = 1, 2, 3), \tag{16}$$

where $\boldsymbol{u}$ is the generalised strain vector whose components $u_i = \boldsymbol{u} \cdot \boldsymbol{d}_i$ relative to the moving frame are the curvatures $(i = 1, 2)$ and the twist $(i = 3)$.

We also introduce a right-handed cylindrical co-ordinate frame $\{\boldsymbol{e}_r, \boldsymbol{e}_\psi, \boldsymbol{e}_z\}$:

$$\begin{aligned} \boldsymbol{e}_r &= \epsilon(\sin\psi \, \boldsymbol{e}_1 - \cos\psi \, \boldsymbol{e}_2), \\ \boldsymbol{e}_\psi &= \epsilon(\cos\psi \, \boldsymbol{e}_1 + \sin\psi \, \boldsymbol{e}_2), \\ \boldsymbol{e}_z &= \boldsymbol{e}_3. \end{aligned} \tag{17}$$

It follows from (15) and (17) that

$$\boldsymbol{e}_r' = \psi' \, \boldsymbol{e}_\psi, \qquad \boldsymbol{e}_\psi' = -\psi' \, \boldsymbol{e}_r, \tag{18}$$

and

$$\boldsymbol{d}_3 = \epsilon \sin\theta \, \boldsymbol{e}_\psi + \cos\theta \, \boldsymbol{e}_z. \tag{19}$$

The balance laws for the internal force $\boldsymbol{F}$ and moment $\boldsymbol{M}$ in the rod are given by (see, e.g., [2])

$$\boldsymbol{F}' + \boldsymbol{p} = \boldsymbol{0}, \tag{20}$$

$$\boldsymbol{M}' + \boldsymbol{r}' \times \boldsymbol{F} = \boldsymbol{0}. \tag{21}$$

Here $\boldsymbol{p}$ is the resultant external force per unit length of rod (pressure) acting on the rod.

For simplicity we shall assume linear and diagonal constitutive relations between the stresses and the strains:

$$\boldsymbol{M} \cdot \boldsymbol{d}_i = K_{ij} u_j \quad (i, j = 1, 2, 3), \qquad K = \text{diag}(B, B, C), \tag{22}$$

where $B$ and $C$ are the bending and torsional stiffnesses, both assumed to be constant. $K_{11} = K_{22}$ because of isotropy. Note that, despite the diagonal stiffness matrix $K$ for a single strand, the ply as a whole will have an effective non-diagonal stiffness matrix due to coupling between the various elastic degrees of freedom (see also Section 6). From (16) and (22) it follows that for the internal moment we can write

$$\boldsymbol{M} = B \, \boldsymbol{d}_3 \times \boldsymbol{d}_3' + C \, u_3 \, \boldsymbol{d}_3. \tag{23}$$

10

Note that this equation extends (22) to a *vectorial* constitutive relation, this being a special property of an isotropic rod.

If we denote the components of force in the cylindrical frame by $\boldsymbol{F} = (F_r, F_\psi, F_z)$ then by (15) we have

$$\boldsymbol{F} \times \boldsymbol{d}_3 = (F_\psi \cos\theta - \epsilon F_z \sin\theta)\, \boldsymbol{e}_r - F_r \cos\theta\, \boldsymbol{e}_\psi + \epsilon F_r \sin\theta\, \boldsymbol{e}_z. \tag{24}$$

Inserting (23) and (24) into the moment balance equation (21) gives the three equations

$$-B\theta'' + B\psi'^2 \sin\theta \cos\theta - Cu_3\psi' \sin\theta = \epsilon F_\psi \cos\theta - F_z \sin\theta, \tag{25}$$

$$\epsilon F_r = B\psi'' \sin\theta + 2B\psi'\theta' \cos\theta - Cu_3\theta', \tag{26}$$

$$Cu_3' = 0. \tag{27}$$

The last equation states that twist, $u_3$, is constant along the rod. Its value will be determined by the boundary conditions.

So far we have not made any assumptions on the shape of the strand. In turning to force balance we now specialise to the case of a helical strand. This means that from now on we assume $\theta = $ const. and $\psi' = (\epsilon/R)\sin\theta$, so that (15) becomes equivalent to (1). $R$ is the radius of the helix. In this case of a helical ply we note that, excepting the case $n = 2$ with $\theta < \pi/4$, each cross-section of a given strand $i$ is acted upon by two neighbouring cross-sections belonging to strands $i - 1$ and $i + 1$. Thus we can express force balance (20) as

$$\boldsymbol{F}' + \boldsymbol{p}_{21} + \boldsymbol{p}_{31} = \boldsymbol{0}, \tag{28}$$

where

$$\boldsymbol{p}_{21}(s) = p_{21}(s)\,\frac{\boldsymbol{r}_1(s) - \boldsymbol{r}_2(s_2)}{|\boldsymbol{r}_1(s) - \boldsymbol{r}_2(s_2)|}, \qquad \boldsymbol{p}_{31}(s) = p_{31}(s)\,\frac{\boldsymbol{r}_1(s) - \boldsymbol{r}_3(s_3)}{|\boldsymbol{r}_1(s) - \boldsymbol{r}_3(s_3)|}. \tag{29}$$

Here $\boldsymbol{p}_{21}$ is the pressure, of magnitude $p_{21}$, strand 2 exerts on strand 1. The shift in arclength implies that $s_2 = s - \epsilon x R$. Similarly, $\boldsymbol{p}_{31}$ is the pressure strand 3 exerts on strand 1, with $s_3 = s + \epsilon x R$. For $n = 2$ and $\theta > \pi/4$ the two touching cross-sections are in fact at different arclengths on the same (opposite) strand (cf. Fig. 1). (When interpreted properly, (28) is also valid for $n = 2$ and $\theta < \pi/4$. In this case the two touching sections are on the same strand and at the same arclength, so $\boldsymbol{p}_{21} = \boldsymbol{p}_{31}$ and hence $\boldsymbol{p} = 2\,\boldsymbol{p}_{21}$; that is to say, there is really only one touching section, counted twice.)

In writing down (29) the pressures are assumed to act normal to the surface of the strands, which amounts to an assumption of frictionless contact. Note that $\boldsymbol{r}_2 = \mathcal{R}_n \boldsymbol{r}_1$ and $\boldsymbol{r}_3 = \mathcal{R}_n^{-1} \boldsymbol{r}_1$. Because our ply is uniform, by symmetry $p_{21} = p_{31} =: p_1$. Straightforward geometry then shows that

$$\boldsymbol{p} = \boldsymbol{p}_{21} + \boldsymbol{p}_{31} = \rho\, p_1 \left( 1 - \cos\left( x \sin\theta - \frac{2\pi}{n} \right) \right) \boldsymbol{e}_r =: p\,\boldsymbol{e}_r. \tag{30}$$

So, even though the strands interact in an intrinsically three-dimensional way and the interstrand pressures are not normal to the ply axis, the total pressure *is* normal to this axis and to the imaginary cylinder on which the strands wind. Consequently, we are within the framework of previous work dealing with the case $n = 2$, $\theta < \pi/4$ [44, 40, 45].

In order to determine the pressure $p$ we make use of force balance (20), which yields

$$F'_r = \frac{\epsilon F_\psi}{R} \sin\theta - p, \tag{31}$$

$$F'_\psi = -\frac{\epsilon F_r}{R} \sin\theta, \tag{32}$$

$$F'_z = 0. \tag{33}$$

For a uniform ply (26) gives $F_r = 0$, so all three force components are seen to be constant. Axial force balance for the overall ply gives

$$F_z = \frac{F_0}{n}, \tag{34}$$

where $F_0$ is the axial force applied to the ply as a whole (positive for tension). $F_\psi$ is found by axial moment balance, which for the overall ply can be expressed as

$$nM_z + nRF_\psi = M_0. \tag{35}$$

Here $M_0$ is the axial moment applied to the ply as a whole, while $M_z$ is the $z$ component of the internal moment in a single strand found by forming the dot product of (23) with $\boldsymbol{e}_z$. We obtain

$$F_\psi = \frac{M_0}{nR} - \frac{\epsilon B}{R^2} \sin^3\theta - \frac{Cu_3}{R} \cos\theta. \tag{36}$$

Then (31) gives for the pressure

$$p = -\frac{B}{R^3} \sin^4\theta - \frac{\epsilon Cu_3}{R^2} \sin\theta\cos\theta + \frac{\epsilon M_0}{nR^2} \sin\theta. \tag{37}$$

This result is in agreement with expressions in [44, 40, 45], but it should be remembered that $R$, instead of simply being equal to $r$, is now given by (4) and (5) in terms of $r$ and $\theta$.

The interstrand pressure $p_1$ can then be obtained from (30):

$$p_1 = \frac{p}{\rho \left[ 1 - \cos\left( x\sin\theta - \frac{2\pi}{n} \right) \right]}, \quad \text{or, by (4),} \quad \frac{p_1}{p} = \frac{\sqrt{2\left[ 1 - \cos\left( x\sin\theta - \frac{2\pi}{n} \right) \right] + x^2\cos^2\theta}}{2\left[ 1 - \cos\left( x\sin\theta - \frac{2\pi}{n} \right) \right]}. \tag{38}$$

It follows that $p$ and $p_1$ have the same sign. Finally, (25), with $\theta'' = 0$ and $\psi' = (\epsilon/R)\sin\theta$, when combined with (36) and (34), gives an equilibrium relation, which in terms of the dimensionless parameters

$$\gamma = \frac{C}{B}, \qquad f = \frac{r^2 F_0}{B}, \qquad m = \frac{rM_0}{B} \tag{39}$$

reads

$$2n\sin^3\theta\cos\theta + \epsilon n\rho\gamma ru_3 \cos 2\theta + \rho^2 f \sin\theta - \epsilon\rho m\cos\theta = 0. \tag{40}$$

12

Using this to eliminate $u_3$ in (37) we find for the dimensionless pressure

$$\frac{pr^3}{B} = \frac{\sin^2 \theta}{n\rho^3 \cos 2\theta} \left( n \sin^2 \theta + \rho^2 f \cos \theta - \epsilon \rho m \sin \theta \right). \tag{41}$$

In a fully *dead* (i.e., force and moment controlled) situation, in which not only $f$ and $m$ but also the twisting moment $\gamma r u_3$ is prescribed, all quantities are determined: (40), (4) and (5) provide three coupled equations for $\theta$, $x$ and $\rho$, and (41) and (38) then give the pressures $p$ and $p_1$. If instead of $u_3$ some other quantity is given (for instance, related to the formation of the ply), then an additional equation must be derived relating it to the present quantities in our formulation. We deal with this in the next section.

**The uniform balanced ply:**
In case no end loads are applied, so that the strands are held together purely by geometrical constraints (as, for instance, in the DNA plasmids considered in [7]), then $f = m = 0$ and (40) and (41) reduce to

$$\epsilon \gamma r u_3 = -\frac{2 \sin^3 \theta \cos \theta}{\rho \cos 2\theta}, \tag{42}$$

$$\frac{pr^3}{B} = \frac{\sin^4 \theta}{\rho^3 \cos 2\theta}. \tag{43}$$

Fig. 6 shows $\rho$, $\gamma r u_3$, $p$ and $p_1$ as a function of $\theta$ for $n = 2$: $\rho$ diverges at $\pi/2$, while $u_3$ and the pressures diverge at $\pi/4$, which is the lock-up angle. For each value of $u_3$ there are two possible angles $\theta$: one smaller than $\pi/4$, one larger than $\pi/4$, with different handedness of the corresponding helix. Note that $p_1$ goes through a maximum along the (dashed) non-trivial branch before reaching $-\pi^2/8$ at $\theta = \pi/2$. At the trivial (solid) branch the final value is $-0.5$. The corresponding limiting values for $p$ are 0 and $-1$, respectively.

Fig. 7 gives the same plots for $n = 3$. Results for $n > 3$ are not qualitatively different from these. The divergence of $u_3$, $p$ and $p_1$ at $\theta = \pi/4$ occurs for all $n$ and is thus found to be unrelated to the lock-up phenomenon at that same angle, as the latter only occurs for $n = 2$. Solutions with $\theta < \pi/4$ have a positive (repulsive) pressure and are therefore physically realistic. However, the negative-pressure solutions for $\theta > \pi/4$ need not be dismissed as unrealistic. Such solutions could provide useful models for plied macromolecules such as DNA or proteins in which attractive interstrand forces are present. The constant pressure would be a smooth approximation of, for instance, discretely distributed hydrogen bonds.

# 4 Plies formed from pretwisted strands

In a realistic loading process $u_3$ is normally unknown and some sort of end angle is imposed instead. Consider, for instance, the following situation. We start with a number (say 3) of straight strands of length $L$ arranged such that their centrelines lie on a cylinder of radius given by (7). While
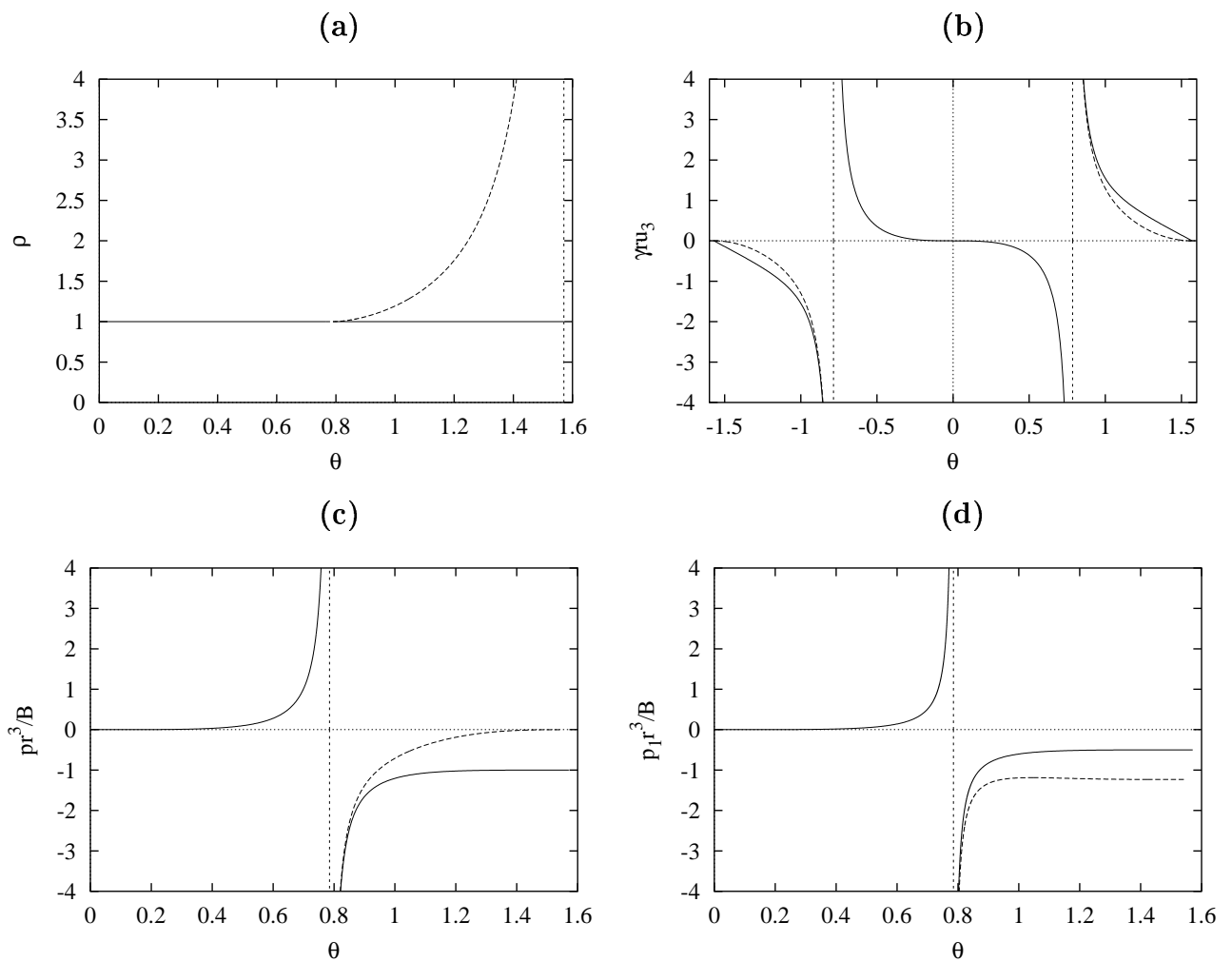
Figure 6: $\rho$, the dimensionless twisting moment $\gamma r u_3$ and the dimensionless pressures as a function of $\theta$ for the balanced 2-ply. The dashed curves represent the non-trivial branch. For $\gamma r u_3$ the left-handed ply solutions are represented by negative $\theta$.

keeping the left-hand ends fixed we turn each of the right-hand ends through a positive angle $\bar{\phi}$, clockwise when looking down the rod from left to right. Next we clip or glue the ends together so that the strands cannot move relative to each other. Finally, we let go of the ends. A natural question to ask is: what is the helical angle $\theta$ of the resulting (almost uniform) 3-ply? (Simple tests with silicone rubber rods show that a uniform ply, modulo some small deviations from uniformity at the ends, is one of the configurations the structure can adopt, branched structures forming other possibilities.)

By introducing a third Euler angle $\phi$ the twist can be written as

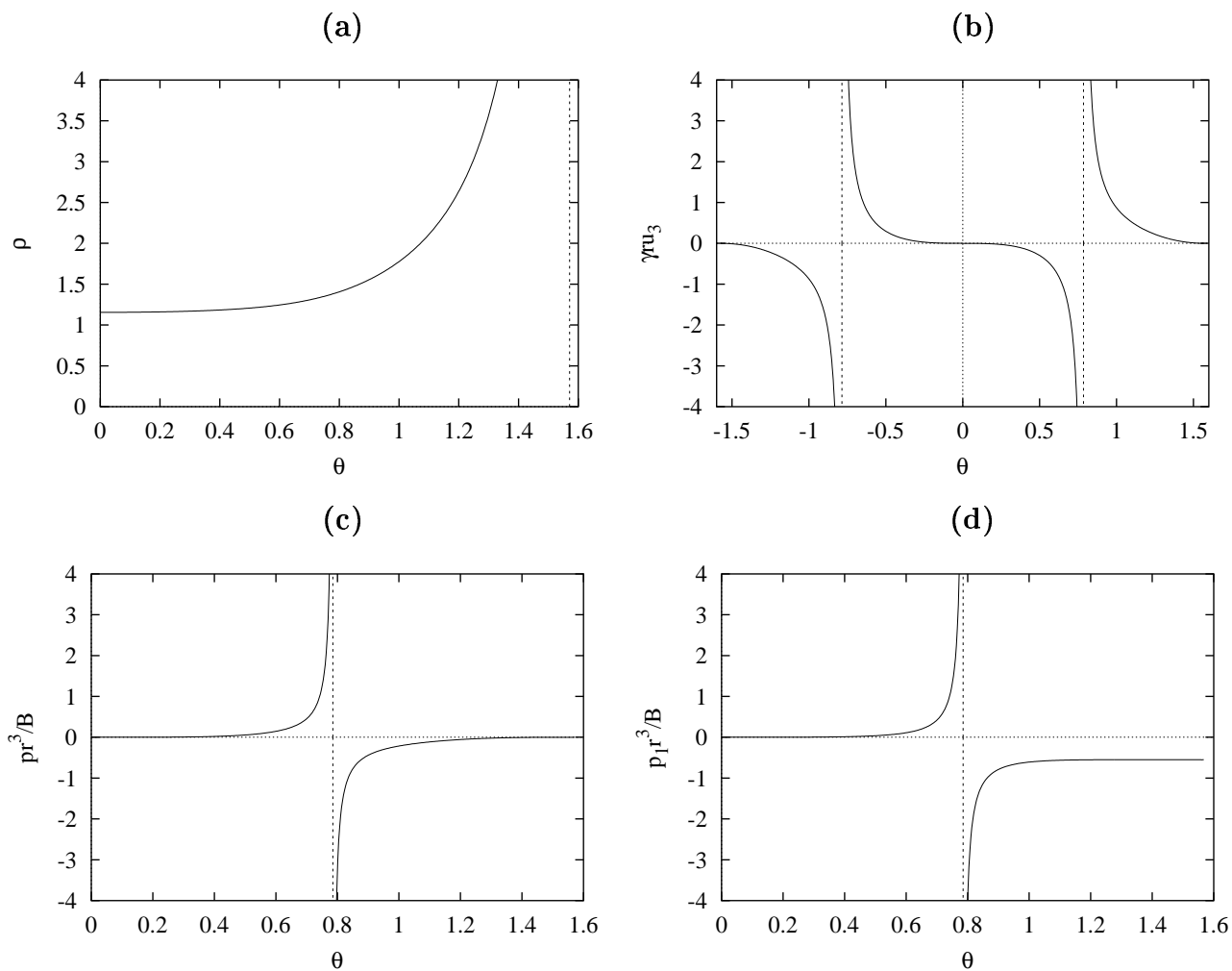$$u_3 = \phi' + \psi' \cos\theta = \phi' + \frac{\epsilon \sin 2\theta}{2R} \tag{44}$$

14

Figure 7: $\rho$, the dimensionless twisting moment $\gamma r u_3$ and the dimensionless pressures as a function of $\theta$ for the balanced 3-ply. For $\gamma r u_3$ the left-handed ply solutions are represented by negative $\theta$.

(see [2, 25]). Since the second term on the right-hand side is precisely the torsion of a helical curve, (44) gives the usual decomposition of twist into space-curve torsion and internal twist, also sometimes called Love's twist. (This interpretation of $\phi'$ as internal twist only holds for constant $\theta$.) Since $\theta$ and $u_3$ are constant, $\phi(s)$ will be a linear function of arclength and $\phi'$ will depend only on the boundary values $\phi(0)$ and $\phi(L)$. The rotation through $\bar{\phi}$ mentioned above puts a right-handed twist $u_{30} = \phi' = (\phi(L) - \phi(0))/L = \bar{\phi}/L$ into each of the (straight) strands. Because of the way the ends of the strands are clipped together the end angles $\phi(0)$ and $\phi(L)$ will not change in the subsequent loading process in which torsion and twist are exchanged (turning the end of the ply changes $\psi$, not $\phi$). We can therefore write (44) as

$$u_3 = \frac{\bar{\phi}}{L} + \frac{\epsilon \sin 2\theta}{2R}. \qquad (45)$$

15

In the Appendix we present an alternative derivation of this result by defining the topological concepts of link and writhe for $n$-plies. Fig. 12 shows two stages in the creation of a balanced 3-ply.

It should be noted that once the strands are released, the end clips will not provide the correct end conditions for a uniform ply. However, we can expect any significant non-uniformity to be localised near the ends. This was indeed very much the experience in [45] for $n = 2$. The error made by assuming a uniform ply is therefore expected to be small.

Combining (45) with (40), and introducing the aspect ratio

$$a = \frac{r}{L}, \tag{46}$$

we arrive at the following equation:

$$2n \sin^3 \theta \cos \theta + \frac{n\gamma}{4} \sin 4\theta + \epsilon n\gamma \bar{\phi} a\rho \cos 2\theta + \rho^2 f \sin \theta - \epsilon \rho m \cos \theta = 0. \tag{47}$$

For a ply with given $\bar{\phi}$ and held by known end loads $f$ and $m$, (4), (5) and (47) define a set of three equations for $\theta$, $x$ and $\rho$. With (47) we can write (41) as

$$\frac{pr^3}{B} = \frac{\sin \theta \tan \theta}{n\rho^3} \left( n(1 - \gamma) \sin^2 \theta \cos \theta - \epsilon n\gamma \bar{\phi} a\rho \sin \theta + \rho^2 f \right), \tag{48}$$

revealing that for fixed $\bar{\phi}$ the pressure has no singularity at $\theta = \pi/4$.

Note that $a$ and $\bar{\phi}$ appear in the equations only in the combination $\bar{\phi} a$. This quantity has the following physical meaning. If we imagine the initial straight and untwisted strands to have stripes painted on their surfaces, parallel to their centrelines, then after putting in the angle $\bar{\phi}$ each stripe forms a right-handed helix. If $\pi/2 - \chi$ is the pitch angle of this helix, then we have

$$\tan \chi = \bar{\phi} a. \tag{49}$$

The angle $\chi$ is the angle between the stripes and the centreline if we imagine the cylindrical surface of the strand to be unrolled. In the numerical results that follow we shall parametrise the link by $\bar{\phi} a$ which we shall call the pretwist, in line with standard terminology in the textile literature [12, 13]. Fig. 8 shows how the ply angle of a balanced ply varies with the pretwist $\bar{\phi} a$. As in the analogous Figs 6(b) and 7(b), for each value of the pretwist there are two possible ply angles, one smaller than $\pi/4$, the other larger than $\pi/4$ (in magnitude). The small-angle (resp. large-angle) solution has a handedness $\epsilon$ opposite (resp. equal) to the sign of the pretwist.

Of particular interest is the case $p_1 = 0$, which defines the onset of strand separation and thereby signals the limit of the ply's proper mechanical functioning. Since $p$ and $p_1$ have the same sign, the condition $p_1 = 0$ is equivalent to $p = 0$. If we eliminate $\theta$ between (47) and (41) we find the locus of $p = 0$ shown in the control spaces of Figs 9 and 10. The former contrasts the high and low pretwist cases for the 2-ply. The straight lines, of slope $\epsilon \rho \tan \theta$, are constant-$\theta$ curves as given by (47) drawn for equal increments of $\theta$. If in an experiment the applied force and moment were varied such that the helical angle $\theta$ stayed the same, then a solid straight line would be followed
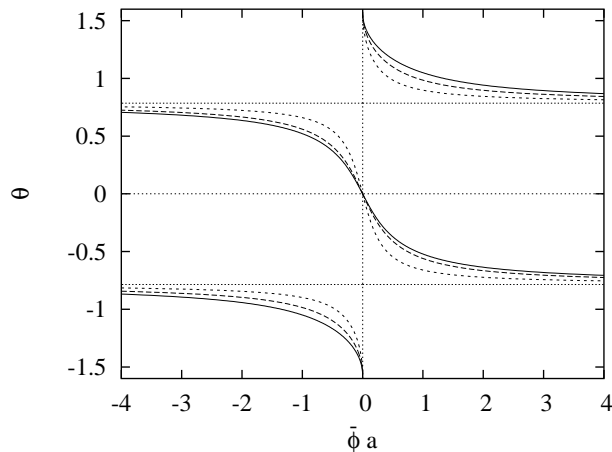
Figure 8: The balanced ply angle $\theta$ against the pretwist $\bar{\phi}a$ for $n = 2$ (solid), $n = 3$ (dashed) and $n = 6$ (dotted). Left-handed ply solutions are represented by negative $\theta$. For each value of the pretwist there are two possible angles, one smaller than $\pi/4$, the other larger than $\pi/4$ (in magnitude). The small-angle helices are left-handed for $\bar{\phi}a > 0$ and right-handed for $\bar{\phi}a < 0$; the converse is true for the large-angle helices. ($\gamma = 3/4$.)

in Fig. 9 up to the point of intersection with the $p = 0$ curve where strand separation would be initiated. Fig. 10 shows the analogous results for the 3-ply for comparison. Note that at $\theta = 0$ the moment is given by $M_0 = nCu_{30} = n\bar{\phi}C/L$, or $m = n\gamma\bar{\phi}a$, the moment with which we hold the ply before we let go.

It should be realised that under compression the ply may undergo Euler buckling before the point of vanishing pressure is reached, especially for long plies. A study of Euler buckling would require the bending stiffness of the overall ply, which is not available in the present work. Another type of instability is the collapse of the ply in case $n > 3$ (see also Section 7).

We end this section with the following important observation. According to Fig. 8, the solution set of *balanced* pretwisted $n$-plies consists of two disconnected branches separated by $\theta = \pi/4$. If one starts with $n$ parallel strands, then no matter how much pretwist $\bar{\phi}a$ one puts into each strand, one will always end up with a ply of angle less than $\pi/4$. In order to create a balanced ply with an angle $\theta > \pi/4$ one must start on the other solution branch. However, by judiciously applying end loads $(f, m)$ one can get from one solution branch to the other: fixing $\bar{\phi}a$ one can follow a path in the load plane of Fig. 9 or 10 that leads one from $\theta < \pi/4$ to $\theta > \pi/4$. Since we are not considering stability of solutions we have to assume here that this manoeuvre can be performed along a stable solution path.

# 5   A variational formulation

The variable length of the ply is given by $L\cos\theta$, while the total rotation of the ply, measured from the datum in which the $n$ strands lie straight side by side, is given by $\psi(L) - \psi(0) = (\epsilon L/R)\sin\theta$.
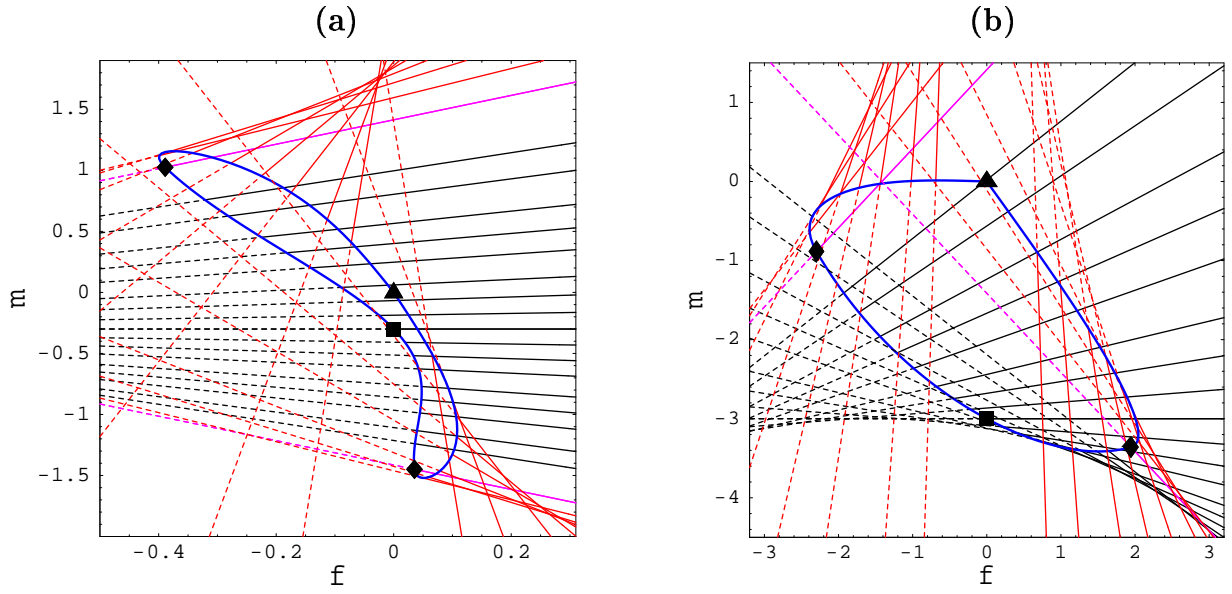
**Figure 9:** Control space of end force, $f$, and end moment, $m$, for a 2-ply of fixed link. (a) is for low pretwist, $\bar{\phi}a = -0.2$, (b) for high pretwist, $\bar{\phi}a = -2.0$. Bold curves are the locus of $p = 0$, shown for both right-handed ($\epsilon = 1$) and left-handed ($\epsilon = -1$) plies. The solid square indicates where $\theta = 0$, the diamonds where $\theta = \pi/4$ and the triangle where $\theta = \pi/2$. The trivial solution is only shown for $\theta < \pi/4$. The straight lines are constant-$\theta$ curves, rising (from left to right) for $\epsilon = 1$, falling for $\epsilon = -1$, and solid for $p > 0$ (potentially stable), dashed for $p < 0$ (unstable). ($\gamma = 3/4$.)
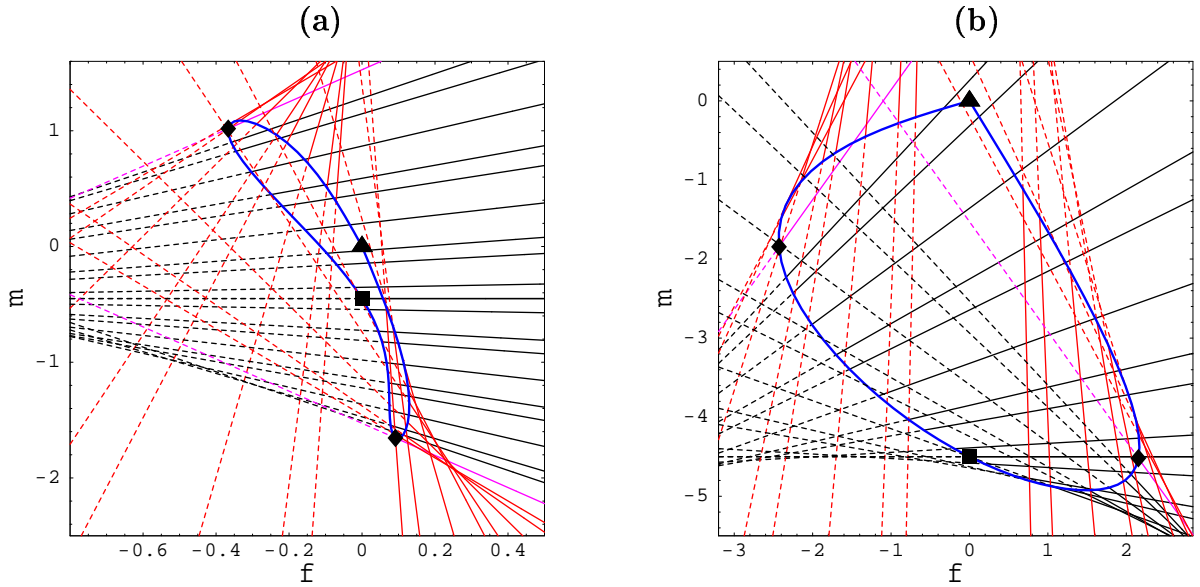


**Figure 10:** Same as Fig. 9 but for the 3-ply.

18

We can therefore introduce the dimensionless *corresponding displacements* through which the end loads $f$ and $m$ do work:

$$d_f = \frac{1}{a} \cos \theta, \tag{50}$$

$$d_m = \frac{\epsilon}{a\rho} \sin \theta. \tag{51}$$

These displacements can be used to give an alternative and more concise derivation of the equilibrium equations for helical strands by means of an energy analysis. We regard $\theta$, $R$, $x$ and the third Euler angle $\phi$ as independent variables, subject to the constraint that there be no self-penetration, i.e., when two sections $\boldsymbol{r}_1(s_1)$ and $\boldsymbol{r}_2(s_2)$ touch then $|\boldsymbol{r}_1(s_1) - \boldsymbol{r}_2(s_2)| = 2r$ (condition C1). The total potential energy of the ply is the sum of the bending energy $U_b$, the torsional energy $U_t$, the work done through the resultant distributed force $p$ (by virtue of the varying radius $R$), $U_p$, and the energy of the end loads $U_l$, given by

$$U_b = \frac{1}{2} nLB\kappa^2, \tag{52}$$

$$U_t = \frac{1}{2} nLCu_3^2, \tag{53}$$

$$U_p = -nLpR, \tag{54}$$

$$U_l = -F_0 d_f r - M_0 d_m = -F_0 L \cos \theta - \frac{\epsilon M_0 L}{R} \sin \theta. \tag{55}$$

Here $\kappa = \sin^2 \theta / R$ is the curvature of the helical rod and $u_3$ the twist, which for uniform $\theta$ can be written as $u_3 = \phi' + (\epsilon/R) \sin \theta \cos \theta$ (cf. (44)). Thus we look for stationary points of the Lagrangian (total potential energy)

$$\mathcal{L}(\theta, R, x, \phi) = \frac{B \sin^4 \theta}{2R^2} + \frac{C}{2} \left( \phi' + \frac{\epsilon \sin \theta \cos \theta}{R} \right)^2 - \frac{F_0}{n} \cos \theta - \frac{\epsilon M_0}{nR} \sin \theta - pR - \lambda R^2 \Delta(\theta, x), \tag{56}$$

where $\lambda$ is a Lagrange multiplier and $\Delta$ is defined in (4).

The Euler-Lagrange equation for $\phi$, $\mathrm{d}/\mathrm{d}s \, (\mathrm{d}\mathcal{L}/\mathrm{d}\phi') = \mathrm{d}\mathcal{L}/\mathrm{d}\phi$, immediately yields (27), expressing that $Cu_3$ is constant. (45) can then be used to identify $\phi$ with the pretwist. The equation for $x$ gives (5), while the equations for $R$ and $\theta$ yield

$$p = -\frac{B}{R^3} \sin^4 \theta - \frac{\epsilon Cu_3}{R^2} \sin \theta \cos \theta + \frac{\epsilon M_0}{nR^2} \sin \theta - 2\lambda R \Delta(\theta, x), \tag{57}$$

$$\frac{2B}{R^2} \sin^3 \theta \cos \theta + \frac{\epsilon Cu_3}{R} \cos 2\theta + \frac{F_0}{n} \sin \theta - \frac{\epsilon M_0}{nR} \cos \theta - \lambda R^2 \frac{\partial \Delta(\theta, x)}{\partial \theta} = 0. \tag{58}$$

The interpretation here is that the loads $F_0$, $M_0$ and $p$ are given, and that $\lambda$ is such that the constraint

$$R^2 \Delta(\theta, x) = 4r^2 \tag{59}$$

is satisfied. For $\lambda = 0$, (57) and (58) are exactly the equilibrium equations (37) and (40). If the pressure $p$ does not have the 'right' value (e.g., if the ply is pressurised), then a residual pressure

proportional to $\lambda$ will act to maintain the constraint (59). Note that the total pressure force would then no longer be normal to the ply axis, as evidenced by the $\lambda$ term in (58), which represents normal moment balance.

For the 2-ply with line contact ($\theta < \pi/4$), the above energy analysis can be readily extended to the case of variable $\theta$ [45]. For the more general ply this is not so straightforward. For instance, in writing down the constraint (59) helical centrelines are explicitly assumed.

# 6    Constitutive behaviour of the $n$-ply

The nonlinear constitutive behaviour associated with torsion and extension of $n$-plies is governed by (47) (or (40) in the case of dead loading), (50) and (51). The *linear* response about the balanced state can be determined as follows. First, write (47) as $G(f, m, \theta) = 0$, where $\rho$ is to be considered as a function of $\theta$. For given loads $f$ and $m$ we can solve this for $\theta = \Theta(f, m)$. The *flexibility matrix* can then be written as

$$
\mathcal{F} = \left(
\begin{array}{cc}
\dfrac{\partial d_f}{\partial f}\bigg|_0 & \dfrac{\partial d_f}{\partial m}\bigg|_0 \\[3mm]
\dfrac{\partial d_m}{\partial f}\bigg|_0 & \dfrac{\partial d_m}{\partial m}\bigg|_0
\end{array}
\right) = \left(
\begin{array}{cccc}
\dfrac{\mathrm{d}d_f}{\mathrm{d}\theta}\bigg|_0 \dfrac{\partial \Theta}{\partial f}\bigg|_0 & \dfrac{\mathrm{d}d_f}{\mathrm{d}\theta}\bigg|_0 \dfrac{\partial \Theta}{\partial m}\bigg|_0 \\[3mm]
\dfrac{\mathrm{d}d_m}{\mathrm{d}\theta}\bigg|_0 \dfrac{\partial \Theta}{\partial f}\bigg|_0 & \dfrac{\mathrm{d}d_m}{\mathrm{d}\theta}\bigg|_0 \dfrac{\partial \Theta}{\partial m}\bigg|_0
\end{array}
\right),
\tag{60}
$$

where the subscript 0 indicates that the derivatives are to be evaluated at $f = m = 0$ and $\theta = \theta_0$, with $\theta_0$ the angle of the balanced ply. To find the required derivatives, write (47) formally as $G(f, m, \Theta(f, m)) \equiv 0$ and differentiate this totally with respect to $f$ and $m$,

$$
\frac{\mathrm{d}G}{\mathrm{d}f} = \frac{\partial G}{\partial f} + \frac{\partial G}{\partial \theta}\frac{\partial \Theta}{\partial f} \equiv 0, \qquad\qquad \frac{\mathrm{d}G}{\mathrm{d}m} = \frac{\partial G}{\partial m} + \frac{\partial G}{\partial \theta}\frac{\partial \Theta}{\partial m} \equiv 0,
\tag{61}
$$

to obtain

$$
\frac{\partial \Theta}{\partial f}\bigg|_0 = -\frac{\rho^2 \sin\theta_0}{\dfrac{\partial G}{\partial \theta}\bigg|_0}, \qquad\qquad \frac{\partial \Theta}{\partial m}\bigg|_0 = \frac{\epsilon\rho \cos\theta_0}{\dfrac{\partial G}{\partial \theta}\bigg|_0}.
\tag{62}
$$

The flexibility matrix then becomes

$$
\mathcal{F} = \frac{1}{\dfrac{\partial G}{\partial \theta}\bigg|_0} \left(
\begin{array}{cc}
\dfrac{\rho^2}{a}\sin^2\theta_0 & -\dfrac{\epsilon\rho}{a}\sin\theta_0\cos\theta_0 \\[3mm]
-\dfrac{\epsilon\rho}{a}\sin\theta_0\cos\theta_0 & \dfrac{1}{a}\cos^2\theta_0
\end{array}
\right).
\tag{63}
$$

We notice that $\mathcal{F}$ is symmetric. The derivative $\partial G/\partial\theta|_0$ is finally found by differentiating (47) and substituting for $\bar{\phi}a$ from the same (47), giving

$$
\frac{\partial G}{\partial \theta}\bigg|_0 = n(\gamma - 1)\cos^2 2\theta_0 + \frac{n}{\cos 2\theta_0} - \left(8\sin^3\theta_0\cos\theta_0 + \gamma\sin 4\theta_0\right)\frac{n}{4\rho}\frac{\mathrm{d}\rho}{\mathrm{d}\theta}\bigg|_0,
\tag{64}
$$

where $\mathrm{d}\rho/\mathrm{d}\theta|_0$ is found from (4) and (5) as

$$\left.\frac{\mathrm{d}\rho}{\mathrm{d}\theta}\right|_0 = \frac{\rho^3 \left(-x^2 \cos^2 \theta_0 + 2x \sin \theta_0 \sin \beta + x^2 \cos \beta + \sin^2 \beta\right) \sin \theta_0 \cos \theta_0}{4 \left(\cos^2 \theta_0 + \sin^2 \theta_0 \cos \beta\right)}, \tag{65}$$

$$\beta = \left(x \sin \theta_0 - \frac{2\pi}{n}\right). \tag{66}$$

In the expressions above $\theta_0$ (and hence $\rho$ and $x$) is still to be viewed as a function of $\bar{\phi}a$. For $n = 2$ and $\theta_0 < \pi/4$ we have $\mathrm{d}\rho/\mathrm{d}\theta|_0 = 0$ (as $\rho = 1$), and series expansion about $\theta_0 = 0$ yields explicitly

$$\begin{pmatrix} \left.\dfrac{\partial d_f}{\partial f}\right|_0 & \left.\dfrac{\partial d_f}{\partial m}\right|_0 \\[2ex] \left.\dfrac{\partial d_m}{\partial f}\right|_0 & \left.\dfrac{\partial d_m}{\partial m}\right|_0 \end{pmatrix} = \begin{pmatrix} \dfrac{1}{2a}\displaystyle\sum_{i=1}^{\infty}\dfrac{a_{i-1}(\gamma)}{\gamma^i}\theta_0^{2i} & -\dfrac{1}{2a}\displaystyle\sum_{i=1}^{\infty}\dfrac{b_{i-1}(\gamma)}{\gamma^i}\theta_0^{2i-1} \\[3ex] -\dfrac{1}{2a}\displaystyle\sum_{i=1}^{\infty}\dfrac{b_{i-1}(\gamma)}{\gamma^i}\theta_0^{2i-1} & \dfrac{1}{2a\gamma}\left(1+\displaystyle\sum_{i=1}^{\infty}\dfrac{c_i(\gamma)}{\gamma^i}\theta_0^{2i}\right) \end{pmatrix}, \tag{67}$$

where $a_k(\gamma)$, $b_k(\gamma)$, $c_k(\gamma)$ are polynomials in $\gamma$ of degree $k$ ($a_0 = b_0 = 1$). We notice that for $\theta_0 = 0$ the torsional flexibility is $\partial d_m/\partial m = 1/(2a\gamma)$, half that of a single strand. The other coefficients vanish with $\theta_0$, as they should for two straight inextensible rods. The negative signs of the non-diagonal terms correspond to the fact that as we pull a ply, we tend to unwind it. The case $\gamma = 1$ is special in that (47) then has the explicit solution $\theta_0 = -(\epsilon/2)\arctan(2\bar{\phi}a)$, which can be used directly in (63). For $n > 2$ expansions similar to those in (67) can be obtained by computing series expansions for $x$ and $\rho$ (by successively computing higher-order derivatives of $x$ and $\rho$ with respect to $\theta$).

We finally derive the effective torsional and axial stiffnesses of the overall ply viewed as a straight rod. The ply twist, $u_{3,\mathrm{ply}}$, and extension, $e_{\mathrm{ply}}$, are defined by

$$u_{3,\mathrm{ply}} = \frac{\epsilon(L/R)\sin\theta}{L\cos\theta} = \frac{1}{r}\frac{d_m}{d_f}, \tag{68}$$

$$e_{\mathrm{ply}} = \frac{L\cos\theta}{L\cos\theta_0} = \frac{a\,d_f}{\cos\theta_0}. \tag{69}$$

The use of the chain rule and (63) give

$$\left.\frac{\partial u_{3,\mathrm{ply}}}{\partial m}\right|_0 = \frac{1}{\left.\dfrac{\partial G}{\partial \theta}\right|_0}\frac{1}{r\cos\theta_0}, \qquad \left.\frac{\partial u_{3,\mathrm{ply}}}{\partial f}\right|_0 = \frac{-\epsilon}{\left.\dfrac{\partial G}{\partial \theta}\right|_0}\frac{\rho\sin\theta_0}{r\cos^2\theta_0}, \tag{70}$$

$$\left.\frac{\partial e_{\mathrm{ply}}}{\partial f}\right|_0 = \frac{1}{\left.\dfrac{\partial G}{\partial \theta}\right|_0}\frac{\rho^2\sin^2\theta_0}{\cos\theta_0}, \qquad \left.\frac{\partial e_{\mathrm{ply}}}{\partial m}\right|_0 = \frac{-\epsilon}{\left.\dfrac{\partial G}{\partial \theta}\right|_0}\rho\sin\theta_0. \tag{71}$$

Defining the effective torsional stiffness $C_{\mathrm{ply}}$ by $M_0 = C_{\mathrm{ply}}u_{3,\mathrm{ply}}$ and the effective axial stiffness

$K_{\mathrm{ply}}$ by $F_0 = K_{\mathrm{ply}} e_{\mathrm{ply}}$, we obtain

$$C_{\mathrm{ply}} = B \cos \theta_0 \left. \frac{\partial G}{\partial \theta} \right|_0 , \tag{72}$$

$$K_{\mathrm{ply}} = \frac{B \cos \theta_0}{R^2 \sin^2 \theta_0} \left. \frac{\partial G}{\partial \theta} \right|_0 , \tag{73}$$

while for the twist-stretch cross-stiffnesses $A_{\mathrm{ply}}$ and $H_{\mathrm{ply}}$ defined by $F_0 = A_{\mathrm{ply}} u_{3,\mathrm{ply}}$ and $M_0 = H_{\mathrm{ply}} e_{\mathrm{ply}}$ we find

$$A_{\mathrm{ply}} = -\frac{\epsilon B \cos^2 \theta_0}{R \sin \theta_0} \left. \frac{\partial G}{\partial \theta} \right|_0 , \tag{74}$$

$$H_{\mathrm{ply}} = -\frac{\epsilon B}{R \sin \theta_0} \left. \frac{\partial G}{\partial \theta} \right|_0 . \tag{75}$$

For non-zero $\theta_0$ these stiffnesses are not simply proportional to $n$ or $B$ (except if $n = 2$ and $\theta_0 < \pi/4$).

# 7   Discussion

Plies with empty central holes will probably not be stable if more than three strands are wound together. However, they can be stabilised by inserting an additional central strand of the right radius $(R - r)$ into the hole. Indeed, keratin and mooring rope, both with $n = 6$, occur in this form. Conversely, one can take a core of certain radius and wrap the strands around it. The radius of the core then determines the ply angle, and one has to solve (4) and (5) with $R$ as given and $\theta$ and $x$ as unknown. As an example, Fig. 11 shows the pressure resultant $p$ and the moment $m$ as a function of the force $f$ for a loaded 'cored' 6-ply with a core radius $R = 2.1r$, corresponding to a helical angle of 20°, a realistic value for engineering rope. For given $f$, $m$ is the moment the loading device has to provide in order to maintain equilibrium. Note that the interstrand pressure $p_1$ no longer follows from (38) as the core will also contribute to the required $p$.

We have computed nonlinear as well as linearised constitutive relations for an $n$-ply in terms of the elastic stiffnesses of its strands. The effective ply stiffnesses, including those for twist-stretch coupling, could be compared against experiments on $n$-plies such as collagen, in the same way as in [38] where such comparisons have been made for supercoiled DNA.

$n$-plies as studied here could be used as building blocks for plies with more complicated cross-sections, as the layered structures considered in [20, 21]. Each component (or layer) could be modelled as a rod (or tube) with effective linear stiffnesses as computed in Section 6, and the components could be coupled by compatibility conditions specifying that the components deform together.
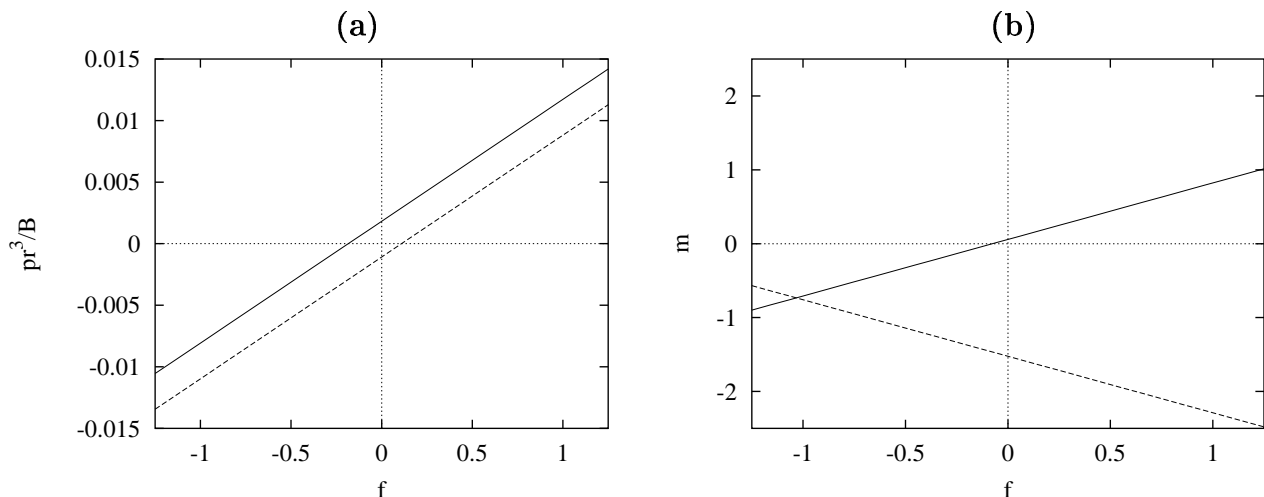
Figure 11: Force-moment characteristics for a loaded cored 6-ply with $\rho = 2.1$, implying $\theta = 20.0°$. Solid lines are for right-handed, dashed lines for left-handed plies. ($\gamma = 3/4$, $\bar{\phi}a = -0.2$.)

# Appendix: link and writhe of an $n$-ply

The linking number, or link, of a rod configuration roughly measures the number of twists that have gone into it in order to create it. Link is usually associated with closed rods. However, by introducing a closure as in [43] we can apply it to open rods as well. (See also [11] for the application of the linking number to open rods, and [37] for a comprehensive study.) This is only necessary for odd $n$; for an even number of strands the ply forms a closed structure, provided we imagine small connecting sections at the ends. For example, for a (clamped) ply created as described in Section 4 we can choose semi-circles of length $\pi r$ for these sections so that the closed centreline is differentiable and the integrals that follow are well-defined. For sufficiently long plies the precise shape of these end sections will not be important. Note that this 'continuation' is entirely natural: in an experiment the employed moulding will essentially do this. Since we are interested in long plies the deviation from uniformity of the clamped ply will be unimportant and we will treat $\theta$ as being constant.

For odd $n$ we imagine the total centreline (running through all the strands of the ply) closed by an additional straight strand of length $L_c$ attached to the ply with the help of further semi-circular sections (see Fig. 12). We shall assume the total closure (straight line plus end sections) to be planar. If the ends of the ply are not exactly aligned then we need to insert, at one end, another small section, say of length $L_i$, between ply and closure in order to obtain a closed structure. This insert can be chosen to be a fraction of a further helical turn. We can imagine the closure to have no torsional stiffness. It will then remain planar in the loading process, and its sole role is to take up the end rotation of the ply. It is a bookkeeping device included so that we can apply the conservation of link for a closed rod. For arbitrary $n$ the total length of the closed centreline can
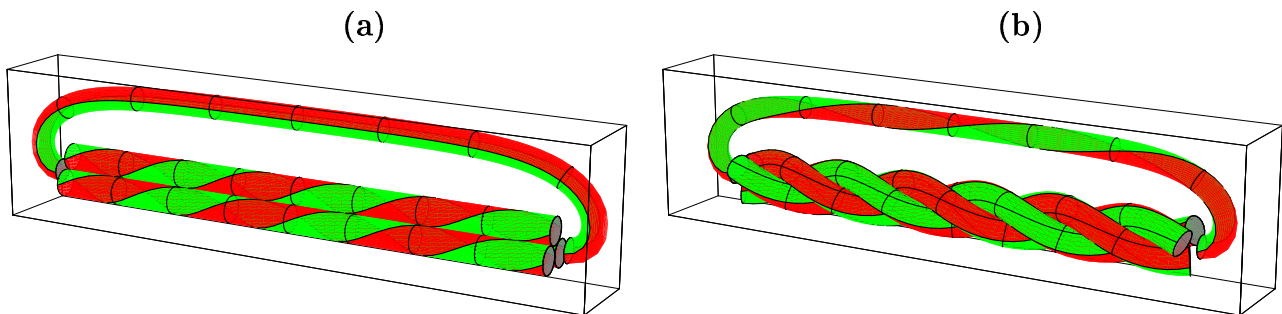
23

Figure 12: A 3-ply with closure illustrating the conservation of link: (a) shows the pretwisted strands, (b) the writhed configuration after releasing the ends. The twist taken up by the planar closure is $T_c = -2.05849 = -\sin\theta/R = -(\psi(L) - \psi(0))$, the negative of the end rotation of the ply. End sections are not shown.

then be written as

$$\mathcal{L} = nL + \sigma(L_c + L_i + \pi r) + n\pi r, \tag{76}$$

where $\sigma = 1$ for $n$ odd and $\sigma = 0$ for $n$ even.

Having thus obtained a closed centreline we can define its linking number, $L_k$. We shall use the celebrated Călugăreanu-White-Fuller formula [4, 47, 14],

$$L_k = T_w + W_r, \tag{77}$$

as its definition. Here $T_w$ is the total (integrated) twist in the rod defined by

$$T_w = \frac{1}{2\pi} \int_0^{\mathcal{L}} u_3 \, \mathrm{d}s, \tag{78}$$

where the origin of arclength has been chosen at one of the ends of the ply, say the left end. $W_r$ is the writhe of the rod and is given by

$$W_r = \frac{1}{4\pi} \int_0^{\mathcal{L}} \int_0^{\mathcal{L}} \frac{[\boldsymbol{r}(s) - \boldsymbol{r}(t)] \cdot [\boldsymbol{r}'(s) \times \boldsymbol{r}'(t)]}{|\boldsymbol{r}(s) - \boldsymbol{r}(t)|^3} \, \mathrm{d}s \, \mathrm{d}t. \tag{79}$$

Note that the writhe is just a property of the shape of the rod's centreline $\boldsymbol{r}$, not of the internal twist, i.e., the rotation of $\boldsymbol{d}_1$ (say) about $\boldsymbol{d}_3$. Fuller [14] showed that the double integral has the interpretation of a signed crossing number averaged over all planar projections. For planar non-self-intersecting curves $W_r = 0$. $L_k$ is a topological invariant: no matter how the strands deform after release of the ends, $L_k$ stays the same. $T_w$ and $W_r$ are not topological invariants; they vary in the loading process. Indeed, by adopting a spatial configuration the initially straight and twisted strands in the ply release torsional energy $(T_w)$ at the expense of bending energy $(W_r)$.

For general shapes the double integral is often difficult to compute. A result by Fuller [15] may then be useful. It makes use of a reference curve and expresses the *difference* of the writhe of the actual curve and the writhe of the reference curve as a single integral. However, choosing a

24

good reference curve (which also has to satisfy a geometric condition) presents its own problems, and since for helical strands the double integrals can be performed explicitly we shall use the definition (79) directly.

The double integral (79) breaks up naturally into a sum of double integrals in which each integral is taken over one of the three different elements making up the ply: a helix (H), an end section (E) or the closure (C). The helical strands can be either forward (running from left to right) or backward (running from right to left). We therefore have to compute the following integrals:

### Helical strand with itself ($W_r^{\mathrm{s}}$)

Using (1) and (15) we obtain for the double integral contribution:

$$4\pi W_r^{\mathrm{s}} = \epsilon\mu \int_0^{\psi_L} \int_0^{\psi_L} \frac{2\left(1 - \cos\Delta\psi\right) - \Delta\psi\sin\Delta\psi}{\left[2\left(1 - \cos\Delta\psi\right) + \mu^2(\Delta\psi)^2\right]^{\frac{3}{2}}} \, \mathrm{d}\psi(s) \, \mathrm{d}\psi(t), \tag{80}$$

where

$$\Delta\psi = \psi(s) - \psi(t), \qquad \psi_L = \psi(L), \qquad \mu = \frac{\cos\theta}{\sin\theta}. \tag{81}$$

With the change of variables

$$x = \frac{\Delta\psi}{2}, \qquad y = \psi(s) + \psi(t), \tag{82}$$

the integral can be rewritten as (see Fig. 13)

$$
\begin{aligned}
4\pi W_r^{\mathrm{s}} &= \epsilon\mu \int_0^{2\psi_L} \int_{-\frac{\psi_L}{2}}^{\frac{\psi_L}{2}} f(x) \, \mathrm{d}y \, \mathrm{d}x - \epsilon\mu \int_0^{\frac{\psi_L}{2}} \int_0^{2x} f(x) \, \mathrm{d}y \, \mathrm{d}x - \epsilon\mu \int_0^{\frac{\psi_L}{2}} \int_{2\psi_L - 2x}^{2\psi_L} f(x) \, \mathrm{d}y \, \mathrm{d}x \\
&\quad - \epsilon\mu \int_{-\frac{\psi_L}{2}}^0 \int_{2\psi_L + 2x}^{2\psi_L} f(x) \, \mathrm{d}y \, \mathrm{d}x - \epsilon\mu \int_{-\frac{\psi_L}{2}}^0 \int_0^{-2x} f(x) \, \mathrm{d}y \, \mathrm{d}x,
\end{aligned}
\tag{83}
$$

where

$$f(x) = \frac{1}{2}\sin x \frac{\sin x - x\cos x}{\left(\sin^2 x + \mu^2 x^2\right)^{\frac{3}{2}}}. \tag{84}$$

We have

$$\int f(x) \, \mathrm{d}x = \frac{1}{2} \frac{x}{\sqrt{\sin^2 x + \mu^2 x^2}}. \tag{85}$$

The singularity at $x = 0$ can be integrated over by using

$$\lim_{x \to \pm 0} \frac{x}{\sqrt{\sin^2 x + \mu^2 x^2}} = \frac{\pm 1}{1 + \mu^2} = \pm\sin\theta. \tag{86}$$

In the limit of a very long ply, $L \to \infty$ (implying $\psi_L \to \infty$ for a right-handed and $\psi_L \to -\infty$ for a left-handed ply), the first integral in (83) then gives the leading-order contribution

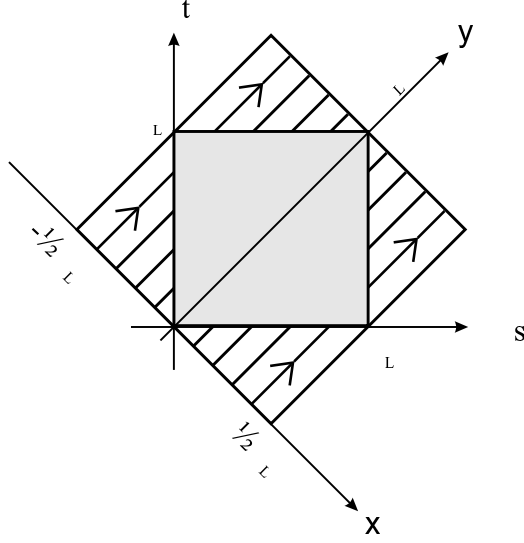$$\epsilon\mu \, 2\psi_L \left(\frac{\epsilon}{\mu} - \epsilon\sin\theta\right) = 2\psi_L(1 - \cos\theta), \tag{87}$$

Figure 13: Integration domain for the double integral $W_r^{\mathrm{s}}$.

valid for both a right-handed and left-handed ply. The other four terms in (83) give

$$-4 \int_0^{\frac{\psi_L}{2}} x f(x) \, \mathrm{d}x + 4 \int_{-\frac{\psi_L}{2}}^0 x f(x) \, \mathrm{d}x. \tag{88}$$

These terms remain bounded in the limit $L \to \infty$ since

$$\int_0^\infty x f(x) \, \mathrm{d}x < \infty. \tag{89}$$

We conclude that for the writhe contribution we have the exact result

$$\frac{2\pi W_r^{\mathrm{s}}}{\psi_L} = 1 - \cos\theta \qquad (L \to \infty). \tag{90}$$

**Helical strand with another helical strand ($W_r^{\alpha\pm}$)**

Now consider two different helical strands, one a $2\pi i/n$-rotated version of the other, running in the same direction. Writing $\psi_1 = \psi(s) = (\epsilon s/R)\sin\theta$, $\psi_2 = \psi(t) = (\epsilon t/R)\sin\theta$ and using (1), (3) and (15) we can write for the writhe contribution:

$$4\pi W_r^{\alpha+} = \epsilon\mu \int_0^{\psi_L} \int_0^{\psi_L} \frac{2\left(1 - \cos(\alpha - \Delta\psi)\right) + \Delta\psi \sin(\alpha - \Delta\psi)}{\left[2\left(1 - \cos(\alpha - \Delta\psi)\right) + \mu^2(\Delta\psi)^2\right]^{\frac{3}{2}}} \, \mathrm{d}\psi_1 \, \mathrm{d}\psi_2, \tag{91}$$

where

$$\Delta\psi = \psi_1 - \psi_2, \qquad \psi_L = \psi(L), \qquad \alpha = 2\pi i/n, \qquad \mu = \frac{\cos\theta}{\sin\theta}, \tag{92}$$

26

and $i$ is an integer between 1 and $n-1$. With the change of variables

$$x = \frac{\Delta \psi}{2}, \qquad y = \psi_1 + \psi_2, \tag{93}$$

the integral can be rewritten as

$$4\pi W_r^{\alpha+} = \epsilon\mu \int_0^{2\psi_L} \int_{-\frac{\psi_L}{2}}^{\frac{\psi_L}{2}} f(x)\, \mathrm{d}x\, \mathrm{d}y - \cdots, \tag{94}$$

where now

$$f(x) = \frac{1}{2} \sin\left(\frac{\alpha}{2} - x\right) \frac{\sin\left(\frac{\alpha}{2} - x\right) + x \cos\left(\frac{\alpha}{2} - x\right)}{\left[\sin^2\left(\frac{\alpha}{2} - x\right) + \mu^2 x^2\right]^{\frac{3}{2}}}. \tag{95}$$

The ellipsis represents the same 'corner' terms as we had for $W_r^{\mathrm{s}}$ above.

We have

$$\int f(x)\, \mathrm{d}x = \frac{1}{2} \frac{x}{\sqrt{\sin^2\left(\frac{\alpha}{2} - x\right) + \mu^2 x^2}}. \tag{96}$$

Note that there is no singularity at $x = 0$. In the limit of a very long ply, $L \to \infty$, the integral in (94) yields

$$\epsilon\mu\, 2\psi_L \frac{\epsilon}{\mu} = 2\psi_L, \tag{97}$$

valid for both right-handed and left-handed plies. The corner terms are again finite and do not contribute in the limit, so we have the exact result

$$\frac{2\pi W_r^{\alpha+}}{\psi_L} = 1 \qquad (L \to \infty). \tag{98}$$

Note that this is independent of $\alpha$, i.e., independent of exactly which pair of helical strands one takes.

For a pair of strands running in opposite directions we find similarly

$$\frac{2\pi W_r^{\alpha-}}{\psi_L} = -1 \qquad (L \to \infty). \tag{99}$$

## Combinations involving end sections or the closure

It is shown in [37] that double integral contributions involving either an end section (E) or the closure (C) remain bounded and therefore can be ignored in the limit $L \to \infty$. The small helical insert required for alignment between ply and closure will contribute at most $2\pi$ (one turn) to $\psi_L$ and can therefore also be ignored in this limit.

We now use the above to evaluate (79) for an even and odd case and then state the general result.

**2-ply**

The 2-ply is built up of two helical strands and two end sections (see the schematic in Fig. 14):

$$\text{Ply} = \text{H}_1^+ \cup \text{E}_{12} \cup \text{H}_2^- \cup \text{E}_{21}.$$

The non-zero contributions to the writhe double integral are tabulated in Table 1. The total writhe is the sum of all the table entries. Thus
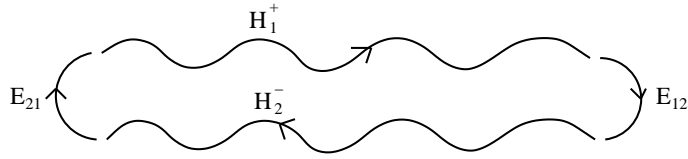
$$W_r = -\frac{2\psi_L}{2\pi}\cos\theta. \tag{100}$$



Figure 14: The components of a 2-ply.

| $2\pi\,W_r$ | $\text{H}_1^+$ | $\text{H}_2^-$ |
|:---:|:---:|:---:|
| $\text{H}_1^+$ | $\psi_L(1-\cos\theta)$ | $-\psi_L$ |
| $\text{H}_2^-$ | $-\psi_L$ | $\psi_L(1-\cos\theta)$ |

Table 1: Writhe contributions for the 2-ply.

**3-ply**

For the 3-ply we have (see Fig. 15)

$$\text{Ply} = \text{H}_1^+ \cup \text{E}_{12} \cup \text{H}_2^- \cup \text{E}_{23} \cup \text{H}_3^+ \cup \text{E}_{3\text{C}} \cup \text{C} \cup \text{E}_{\text{C}1}.$$

From Table 2 we find

$$W_r = \frac{\psi_L}{2\pi}(1 - 3\cos\theta). \tag{101}$$

**General $n$-ply**

In fact, one easily verifies that for general $n$ we get

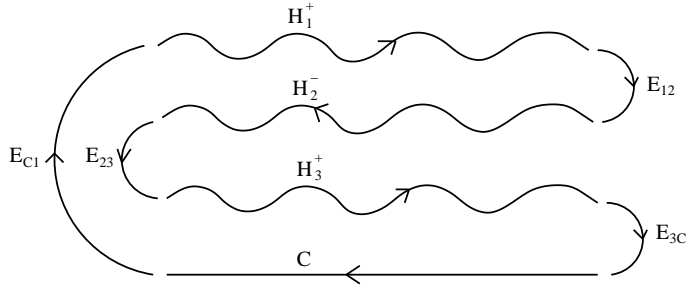$$W_r = \frac{\psi_L}{2\pi}\left(\sigma - n\cos\theta\right) = \frac{\epsilon\,L}{2\pi R}\sin\theta\left(\sigma - n\cos\theta\right). \tag{102}$$

28

Figure 15: The components of a 3-ply with closure.

| $2\pi\,W_r$ | $\mathrm{H}_1^+$ | $\mathrm{H}_2^-$ | $\mathrm{H}_3^+$ |
|---|---|---|---|
| $\mathrm{H}_1^+$ | $\psi_L(1-\cos\theta)$ | $-\psi_L$ | $\psi_L$ |
| $\mathrm{H}_2^-$ | $-\psi_L$ | $\psi_L(1-\cos\theta)$ | $-\psi_L$ |
| $\mathrm{H}_3^+$ | $\psi_L$ | $-\psi_L$ | $\psi_L(1-\cos\theta)$ |

Table 2: Writhe contributions for the 3-ply.

For $n=1$ this result agrees with the writhe of a helix (with closure) as derived in [14].

We now collect all the contributions on the right-hand side of (77). For arbitrary $n$ we can write

$$L_k = T_w + \sigma T_c + W_r, \tag{103}$$

where $T_w$ is the usual total twist in the $n$ strands, and $T_c$ the total twist in the closure (for odd $n$). This latter twist is simply the reverse of the end rotation, $\psi(L) - \psi(0)$, of the ply as a whole. According to (1) this gives

$$T_c = -\frac{\epsilon L \sin\theta}{2\pi R}. \tag{104}$$

If we insert (102) and (104) into (103) the $\sigma$ terms nicely cancel and we obtain

$$L_k = T_w - \frac{\epsilon n L}{2\pi R}\sin\theta\cos\theta, \tag{105}$$

valid for all $n$.

For the pretwisted plies considered in Section 4 the link is given by

$$L_k = \frac{n u_{30} L}{2\pi} = \frac{n\bar\phi}{2\pi}. \tag{106}$$

By combining (106) with (105) and (78) we obtain for the local twist (provided $r/L \ll 1$)

$$u_3 = \frac{\bar\phi}{L} + \frac{\epsilon\sin 2\theta}{2R}, \tag{107}$$

in agreement with (45).

29

# Acknowledgements

# References

[1] J.F. Allemand, D. Bensimon, R. Lavery & V. Croquette, Stretched and overwound DNA forms a Pauling-like structure with exposed bases, *Proc. Natl. Acad. Sci. USA* **95**, 14152-14157 (1998).

[2] S.S. Antman, *Nonlinear Problems of Elasticity* (Springer-Verlag, New York, 1995).

[3] U. Bockelmann, B. Essevaz-Roulet & F. Heslot, DNA strand separation studied by single molecule force measurements, *Phys. Rev. E* **58**, 2386-2394 (1998).

[4] G. Călugăreanu, Sur les classes d'isotopie des nœuds tridimensionnels et leurs invariants, *Czechoslovak Mathematical Journal* **11**, 588-625 (1961).

[5] A. Cardou & C. Jolicœur, Mechanical models of helical strands, *ASME Appl. Mech. Rev.* **50**, 1-14 (1997).

[6] C.R. Chaplin, Torsional failure of a wire rope mooring line during installation in deep water, *Eng. Failure Anal.* **6**, 67-82 (1998).

[7] B.D. Coleman & D. Swigon, Theory of supercoiled elastic rings with self-contact and its application to DNA plasmids, *J. Elasticity* **60**, 173-221 (2000).

[8] G.A. Costello, *Theory of Wire Rope, 2nd ed.* (Springer-Verlag, New York, 1997).

[9] E.H. Dill, Kirchhoff's theory of rods, *Arch. Hist. Exact Sci.* **44**, 1-23 (1992).

[10] B. Essevaz-Roulet, U. Bockelmann & F. Heslot, Mechanical separation of the complementary strands of DNA, *Proc. Natl. Acad. Sci. USA* **94**, 11935-11940 (1997).

[11] B. Fain, J. Rudnick & S. Östlund, Conformations of linear DNA, *Phys. Rev. E* **55**, 7364-7368 (1997).

[12] W.B. Fraser & D.M. Stump, The equilibrium of the convergence point in two-strand yarn plying, *Int. J. Solids Struct.* **35**, 285-298 (1998).

[13] W.B. Fraser & D.M. Stump, Twist in balanced-ply structures, *J. Text. Inst.* **89**, 485-497 (1998).

[14] F.B. Fuller, The writhing number of a space curve, *Proc. Natl. Acad. Sci. USA* **68**, 815-819 (1971).

[15] F.B. Fuller, Decomposition of the linking of a closed ribbon: a problem from molecular biology, *Proc. Natl. Acad. Sci. USA* **75**, 3557-3561 (1978).

[16] D.E. Gilbert & J. Feigon, Multistranded DNA structures, *Curr. Opin. Struct. Biol.* **9**, 305-314 (1999).

[17] O. Gonzalez & J.H. Maddocks, Global curvature, thickness, and the ideal shapes of knots, *Proc. Natl. Acad. Sci. USA* **96**, 4769-4773 (1999).

[18] O. Gonzalez, J.H. Maddocks & J. Smutny, Curves, circles, and spheres, *Contemporary Mathematics* **304**, 195-215 (2002).

[19] J.W.S. Hearle & A.E. Yegin, The snarling of highly twisted monofilaments. Part I: The load-elongation behaviour with normal snarling, *J. Text. Inst.* **63**, 477-489 (1972); Part II: Cylindrical snarling, *J. Text. Inst.* **63**, 490-501 (1972).

[20] W. Jiang, A general formulation of the theory of wire ropes, *ASME J. Appl. Mech.* **62**, 747-755 (1995).

[21] W.G. Jiang, J.L. Henshall & J.M. Walton, A concise finite element model for three-layered straight wire rope strand, *Int. J. Mech. Sci.* **42**, 63-86 (2000).

[22] C. Kang, X. Zhang, R. Ratliff, R. Moyzis & A. Rich, Crystal structure of four-stranded *Oxytricha* telomeric DNA, *Nature*, **356**, 126-131 (1992).

[23] V. Katritch, W.K. Olson, P. Pierański, J. Dubochet & A. Stasiak, Properties of ideal composite knots, *Nature* **388**, 148-151 (1997).

[24] T. Kunoh & C.M. Leech, Curvature effects on contact position of wire strands, *Int. J. Mech. Sci.* **27**, 465-470 (1985).

[25] A.E.H. Love, *A Treatise on the Mathematical Theory of Elasticity, 4th ed.* (Cambridge University Press, Cambridge, 1927).

[26] A. Maritan, C. Micheletti, A. Trovato & J.R. Banavar, Optimal shapes of compact strings, *Nature* **406**, 287-290 (2000).

[27] M. Moakher & J.H. Maddocks, A double-strand elastic rod theory, preprint Institut Bernoulli, Ecole Polytechnique Fédérale de Lausanne, Lausanne, Switzerland (2002).

[28] D.A.D. Parry & J.M. Squire (eds), Fibrous proteins (special issue), *J. Struct. Biol.* **122** (1998).

[29] M. Peyrard & A.R. Bishop, Statistical mechanics of a nonlinear model for DNA denaturation, *Phys. Rev. Lett.* **62**, 2755-2758 (1989).

[30] P. Pierański, In search of ideal knots, in: [35], pp. 20-41.

[31] S. Przybyl & P. Pierański, Helical close packings of ideal ropes, *Eur. Physical J. E* **4**, 445-449 (2001).

[32] I. Rouzina & V.A. Bloomfield, Force-induced melting of the DNA double helix 1: Thermodynamic analysis, *Biophys. J.* **80**, 882-893 (2001); 2: Effect of solution conditions, *Biophys. J.* **80**, 894-900 (2001).

[33] A. Sarkar, J.-F. Léger, D. Chatenay & J.F. Marko, Structural transitions in DNA driven by external force and torque, *Phys. Rev. E* **63**, 051903 (2001).

[34] T. Simonsson, G-quadruplex DNA structures – variations on a theme, *Biol. Chem.* **382**, 621-628 (2001).

[35] A. Stasiak, V. Katritch & L.H. Kauffman (eds), *Ideal Knots*, Series on knots and everything, Vol. 19 (World Scientific, Singapore, 1998).

[36] A. Stasiak & J.H. Maddocks, Best packing in proteins and DNA, *Nature* **406**, 251-253 (2000).

[37] E.L. Starostin, On the writhe of non-closed curves, preprint Institut Bernoulli, Ecole Polytechnique Fédérale de Lausanne, Lausanne, Switzerland (2002) (available at `arXiv:physics/0212095`).

[38] T.R. Strick, J.-F. Allemand, D. Bensimon, A. Bensimon & V. Croquette, The elasticity of a single supercoiled DNA molecule, *Science* **271**, 1835-1837 (1996).

[39] D.M. Stump, W.B. Fraser & K.E. Gates, The writhing of circular cross-section rods: undersea cables to DNA supercoils, *Proc. R. Soc. Lond. A* **454**, 2123-2156 (1998).

[40] J.M.T. Thompson, G.H.M. van der Heijden & S. Neukirch, Super-coiling of DNA plasmids: the mechanics of the generalised ply, *Proc. R. Soc. Lond. A* **458**, 959-985 (2002).

[41] L.R.G. Treloar, The geometry of multy-ply yarns, *J. Text. Inst.* **47**, T348-T368 (1956).

[42] P.N.T. Unwin & P.D. Ennis, Two configurations of a channel-forming membrane protein, *Nature* **307**, 609-613 (1984).

[43] G.H.M. van der Heijden & J.M.T. Thompson, Helical and localised buckling in twisted rods: a uniform analysis of the symmetric case, *Nonlinear Dynamics* **21** 71-99 (2000).

[44] G.H.M. van der Heijden, The static deformation of a twisted elastic rod constrained to lie on a cylinder, *Proc. R. Soc. Lond. A* **457**, 695-715 (2001).

[45] G.H.M. van der Heijden, J.M.T. Thompson & S. Neukirch, A variational approach to loaded ply structures, *Journal of Vibration and Control* **9**, 175-185 (2003).

[46] K.M. Vasquez, L. Narayanan, P.M. Glazer, Specific mutations induced by triplex-forming oligonucleotides in mice, *Science* **290** 530-533 (2000).

[47] J.H. White, Self-linking and the Gauss integral in higher dimensions, *Am. J. Math.* **91**, 693-728 (1969).

[48] M. Yeager & B.J. Nicholson, Structure of gap junction intercellular channels, *Curr. Opin. Struct. Biol.* **6**, 183-192 (1996).